Modelling and control of Cyber-Physical and Human Systems in an office building

Siva Subramanian Swaminathan

Master of Science Thesis

TU Delft Delft University of Technology

Delft Center for Systems and Control

Modelling and control of Cyber-Physical and Human Systems in an office building

Master of Science Thesis

For the degree of Master of Science in Systems and Control at Delft University of Technology

Siva Subramanian Swaminathan

October 31, 2017

Faculty of Mechanical, Maritime and Materials Engineering (3mE) · Delft University of Technology

The work in this thesis was supported by Rijksvastgoedbedrijf and The Green Village. Their cooperation is hereby gratefully acknowledged.

Delft University of Technology
Department of
Delft Center for Systems and Control (dcsc)

The undersigned hereby certify that they have read and recommend to the Faculty of Mechanical, Maritime and Materials Engineering (3mE) for acceptance a thesis entitled

Modelling and control of Cyber-Physical and Human Systems in an office building

by

Siva Subramanian Swaminathan

in partial fulfillment of the requirements for the degree of

Master of Science Systems and Control

Dated: October 31, 2017

Supervisor(s):

dr.ir. Simone Baldi

Reader(s):

dr.ir. Manuel Mazo Jr.

Dr. R. Ferrari

Acknowledgements

First of all, I would like to start by thanking my supervisor, Simone Baldi for giving me the opportunity to work on this thesis. This work would not have been possible without his constant assistance and ideas when I was stuck with a problem.

I would also like to thank Sricharan, Jayesh, Abhimanyu and Divyam for the various discussions we have had over the course of this thesis. This work would not have been possible without your constant feedback. Vaibhav, Siddharth, Nupur, Shubhankar, Novy and many more who I have not mentioned here, thank you for making my journey at TU Delft a wonderful experience.

Bhavna, Ibrahim, Sathya, thank you guys for being there through the ups and downs. It's not been an easy ride and its difficult to fathom how I would have reached so far without your support.

I would like to reserve my last bit of thanks to my family. Amma, Appa and Raghu, your support through all these years is greatest gift anyone has ever given me.

Delft, University of Technology
October 31, 2017

Siva Subramanian Swaminathan

Abstract

Heating, Ventilation and Air-Conditioning (HVAC) units in commercial buildings account for a huge portion of global energy consumption. There is an ever growing need to optimize the energy consumption of an HVAC system along with a system-of-subsystems entity that must be accurately integrated and controlled by the building automation system to ensure the occupants' comfort with reduced energy consumption.

To achieve these goals, it is necessary that accurate models be developed that describe the internal dynamics of the system to employ a satisfactory control architecture. This thesis work aims at provide sufficiently accurate models which are able to estimate the temperature, humidity and CO_2 dynamics in an occupied room. A simplified linear model which describes the dynamics was developed by reformulating the physical equations into a linear regression format. This was followed by the employment of a suitable identification technique to estimate the physical parameters of the system.

The second part of this thesis involves the formulation of a two level control architecture to optimize comfort and energy. In this work we propose a model-based framework to maximize the comfort of the occupants using the Predicted Mean Vote (PMV) index. In particular, the set-point control is based on a predictive controller based on a joint optimization of PMV and energy consumption; the low-level Proportional Integral HVAC controllers are autotuned based on simulations of a thermal model. A simulation based validation via a three room test case is presented: the results show the potential for good temperature tracking with a high degree of comfort while also reducing overall energy consumption.

"A learning experience is one of those things that says, 'You know that thing you just did? Don't do that."

— *Douglas Adams, The Salmon of Doubt*

Contents

List of Figures

Chapter 1

Introduction

Heating, Ventilation and Air-Conditioning (HVAC) systems, widely used in residential and commercial buildings, are responsible for a large part of the global energy consumption [7]. According to the EC's Joint Research Center, Institute for Energy (2009), HVAC systems in the European Union member states were estimated to account for approximately 313 TWh of electricity use in 2007, about 11% of the total 2800 TWh consumed in Europe that year [8]. Energy savings in HVAC systems was therefore identified as a key element to fulfill the target of reducing energy consumption by 20% by 2020. Increased attention has been focused on the reduction of HVAC energy costs while catering to comfort requirements [9] in the form of more efficient equipment [10, 11, 12], novel approaches to HVAC energy storage [13] or supervisory control techniques [14, 15, 16].

In this chapter, we introduce the typical modelling and control techniques employed in state of the art HVAC systems and describe its limitations. We organize this chapter as follows: Section 1-1 gives a brief introduction to climate control in conventional office buildings. Section 1-2 presents the state-of-the-art research that exist in HVAC modelling and control. Section 1-3 summarizes the research objectives and contributions of this MSc thesis and finally Section 1-4 concludes this chapter by presenting the outline of the proposed work.

1-1 Climate control in office buildings - an introduction

Occupancy based control of HVAC systems has gained increased attention over the coming years. This tends to ensure that the user is considered as a part of the control loop rather than an external factor which influences HVAC control, with an example demonstrated in 1-2.

Out of these factors shown in Figure 1-2, Temperature, Humidity and CO_2 are important thermodynamic variables in commercial air conditioning. On a large scale, they influence the rate of biochemical reactions, and thereby contribute to overall comfort of the occupant. In general HVAC applications and literature, modelling and control is mostly based around controlling the indoor temperature of the room while ignoring the control of humidity and

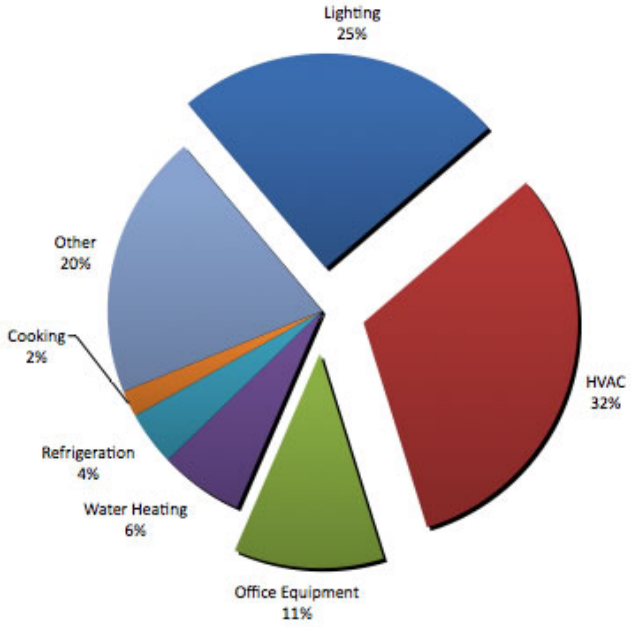

Figure 1-1: Breakdown of energy consumption in commercial buildings [1]

CO_2, or in general, assuming that they would be regulated or stay within predetermined bounds. This could lead to a suboptimal comfort level of the occupants. This necessitates a need to decouple and formulate a model structure these dynamics individually in an occupant zone. Once, decoupling for this is achieved, it would be possible to use any of the widely available control strategies to ensure that these can be controlled effectively.

1-2 Testbeds - Rijkswaterstaat and 3mE, TU Delft - A brief overview

The models outlined in this thesis were initially developed for the Rijskwaterstaat building located in Rijswijk as a part of the Program Green Technologies (PGT 3.0) to understand occupant behaviour and optimize the HVAC system for enhanced control.

The testbed is equipped with a Variable Air Volume (VAV) based HVAC system which takes care of the heating and cooling loads for all the occupants in the building. All occupant rooms and common areas are equipped with a inidividual VAV boxes to control each of the thermal zones according to the occupant's demands. Moreover, as a part of the research program, all rooms in the seventh floor of the testbed is equipped with temperature, humidity, CO_2 and occupancy sensors. The current control strategy in the building consists of PI controllers to control all the components within the HVAC system.

Figures 1-4 and 1-5 show a simplified schematic of a single zone VAV system, similar to the one emloyed in the Rijkswaterstaat testbed. In this system, exhaust air from the room is pumped out using a Return air pump. A portion of this is ventilated out to the external atmosphere and another portion is mixed with inlet air from the atmosphere. The percentage of return air that is mixed with the incoming outside is decided based on the temperature of this return

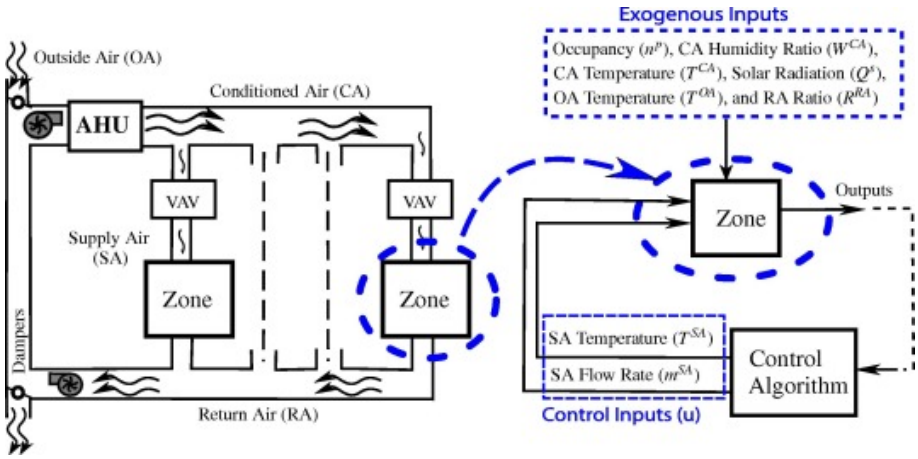

Figure 1-2: Zone level comfort control architecture [2]

Figure 1-3: The Rijkswaterstaat Rijswijk Testbed

air and are regulated using dampers. Depending on the demand and current conditions within the room, air is heated or cooled using heating or cooling coils respectively. These heating or cooling coils are usually gas powered although the current trend is increasingly shifting towards electric heaters. Once the air has been sufficiently heated/cooled, it is sent in to the room where the flow is finally regulated using a VAV unit. The air flow regulation of the VAV is ultimately dependent upon the internal temperature of the room and the temperature differential between the current set-point and instantaneous room temperature. Further detailed information about the working of VAV HVAC systems is detailed in the Appendix.

For the sake of validation of these models and since there was unavailability of data from Rijkswaterstaat, some of the proposed models in this thesis are evaluated using data from the 3mE (Faculty Mechanical, Maritime and Materials Engineering) building. The classroom facility in the building consists of a setup similar to the testbed available in Rijswijk, with the

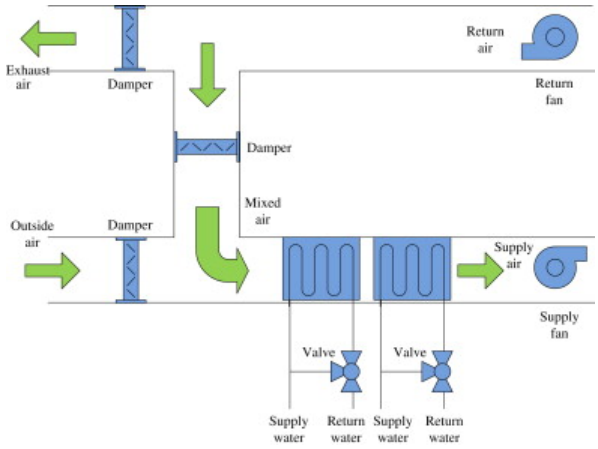

Figure 1-4: Single Zone VAV System -Air Handling Unit level [3]

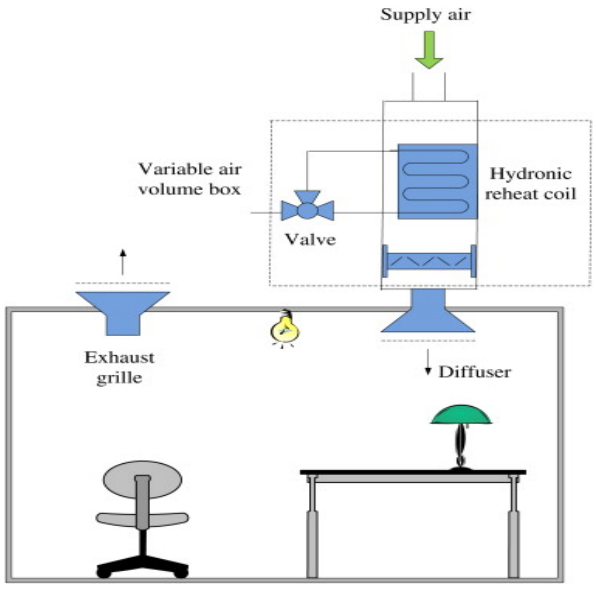

Figure 1-5: Single Zone VAV System -Room level [3]

exception that there are no CO_2, humidity and occupancy data available and different physical characteristics. The control system architecture and Building Management System (BMS) for the HVAC system at 3mE is provided by Johnson Controls, with a sample interface as shown in Figure 1-6. The temperature dynamics models that were developed for the Rijkswaterstaat testbed were retrofitted and modified according to the measurements available in TU Delft and shall be clearly detailed in the following chapters.

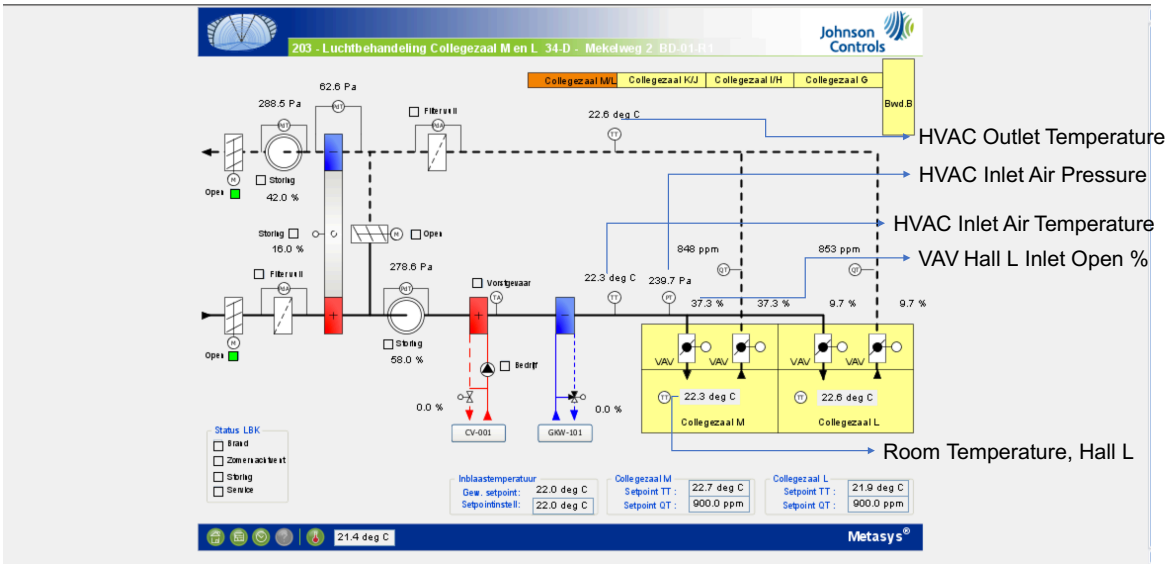

Figure 1-6: Screen shot of Building Management System interface

1-3 State of the art

1-3-1 Modelling techniques

While there exists extensive literature on the modelling of HVAC systems, they are almost always based on the on modelling of thermal dynamics of the system. However, dynamics of other variables such as humidity and CO_2, factors that are almost as equally important as temperature, are largely ignored or are considered as a band that is assumed not to be violated.

Modelling and identification of general HVAC dynamics have been discussed extensively in literature. Most of these fall under 3 main categories: black box modelling, where no physical information of the physics of the system is available; white box modelling, where complete information of the physics of the system is available; grey box modelling, which falls in between these two approaches and the physical parameters are obtained using appropriate system identification techniques.

HVAC system generally comprise of multiple subsystems, such as boilers, chillers, cooling and heating coils, pumps, Air Handling Units (AHUs), Variable Air Volume (VAV) boxes, pipes and ducts. Due to inherent complexities in the overall modelling of these subsystems, designers generally tend to model these subsystems individually, and overall, using black box techniques. With the advent of powerful computing tools and techniques such as machine learning, increasing amount of research is focused on data mining with techniques such as Support Vector Machines (SVMs) and Artificial Neural Networks (ANNs) [17] [18] [19]. They also have the ability to model complex non-linear relationships between the inputs and the outputs, mimicking the kind of relationships that exist in the real world. The other primary model structure used in blackbox modelling comes under the family of multavariable regression, under which there exists Autoregressive exogenous (ARX), Autoregressive moving average exogenous (ARMAX), Autoregressive integrated moving average, Finite Impulse Re-

sponse (FIR), Box Jenkins (BJ) and Output Error (OE) models. [20] compared these model structures to identify the humidity and temperature models of a building over various seasons, where the BJ model outperformed the ARX and ARMAX model.

Recent advancements in identification and modelling techniques has resulted in users modelling these systems with a greybox framework. Greybox models typically provide better accuracy than whitebox models and also require lesser datapoints than blackbox models. However, since these models require knowledge of physics of the building and measurement datasets, they are generally the hardest to be developed out of the three. The most commonly used framework for greybox modelling is the Resistance Capacitance (RC) method where the physical parameters of the building such as thermal resistance and conductance and made analogous to an electrical circuit. [21] developed a RC based modelling structure for a 3 room test, modelling the physical parameters of the building such as wall temperature and window temperature as states of the system. [22] developed a lumped capacitance model of a room using energy balance equations. [23] extended this framework to a polynomial regression with an ARMAX structure to describe the room temperature of the model. [24] extended this modelling framework even further to develop mass balance equations for the description of humidity and CO_2 dynamics. Both these works converted a continuous time model developed using thermodynamics equations and discretized them to create a linear regression model which was then identified using suitable techniques. These structures gave an intuitive understanding of the physics of the system while also providing the advantage that existing identification structures could be used to identify physical parameters.

1-3-2 Control techniques

The second part of this thesis proposed an integrated control framework which can be applied the models developed in the first half to have a control system that is both energy efficient, and for the sake of this work, centered around the user.

Typically, thermal comfort is only defined through a band of temperature that is not to be violated. This generally means that the control input tries to track the lower or upper bounds of this band to ensure other energy minimization and other applicable objectives are optimized. However, as thermal comfort of the users is season dependent and highly subjective, recent research has focused towards quantifying this comfort according to the physical characteristics of both the occupants and their surroundings. The most widely used among these are the Adaptive Comfort Model [25] and the Predicted Mean Vote (PMV) [26], where the latter is more suited in the absence of natural ventilation.

Furthermore, while there exist many intelligent control algorithms, these require the deployment of a completely new control system capable of handling their computational demands, thereby increasing overhead costs. However, most of the HVAC low-level controllers commissioned in the field today, including the test case in this paper are of Proportional-Integral-Derivative (PID) type. Therefore, there exists a need to integrate modern controllers with existing PID controllers to ensure that the control objectives are met. Much of current research in Building Management Systems (BMS) have turned towards Model Predictive Controllers (MPC) for optimal control of building systems. MPCs generally tend to be well posed for such problems: they can handle external disturbances [27]; can handle both linear and nonlinear

models [28] [29], with multiple constraints. This structure allows the facilitation of thermal comfort indices into the cost function along with energy minimization.

1-4 Research questions

Based on the above state of the art, it is clear that there exist various way to model and control HVAC systems in commercial buildings. The main criteria that were used to choose an approach in this thesis are:

- Scalability: The modelling and control technique employed should be easily scalable to multiple rooms.
- Low order: The model developed should be linear and low order to facilitate control design while not at the expense of reducing the overall accuracy of the prediction.
- Occupant-oriented design: The controller should be oriented around maximizing comfort of the user while also decreasing the overall energy consumption of the HVAC system.

With these considerations and available literature, the following research questions were posed as a statement of this thesis:

1. Is it possible to reformulate the nonlinear dynamics of temperature, humidity and CO_2 in a linear way so that linear identification techniques can be implemented, sometimes even in the absence of input measurements?
2. Can a control strategy be developed based on the developed models whose control action is based on the external weather conditions and thermal comfort of the users?
3. Can the control strategy be customized for occupant in each room so that rooms are heated/cooled only when the occupant is present in the room?

1-5 Outline of the thesis

In the forthcoming chapters, various techniques possible to model and control building systems will be discussed.

Chapter 2 discusses the physics that describes the dynamical evolution of the variables and formulates a linear model using mass balance and energy balance equations.

Chapter 3 describes the ARMAX based greybox identification procedure that was employed in obtaining the parameters of the temperature dynamics of the system.

Chapter 4 discusses the concept of an integrated control framework and presents the simulation results.

Chapter 5 presents conclusions from the research that was carried out and future recommendations on this work.

Chapter 2

Occupant-oriented modelling of building dynamics

This chapter is organized as follows, Section 2-1 discusses the assumptions and simplifications that were considered for modelling the dynamics. Section 2-2 gives a brief introduction to the physical principles that govern thermal modelling of building. Section 2-3 details the modelling approach for temperature dynamics. Section 2-4 discusses the modelling approach for humidity dynamics. Section 2-5 discusses the modelling approach for CO_2 dynamics. Section 2-5 summarizes and concludes the results from the chapter and sets the base for the identification procedure for the forthcoming chapter.

2-1 Modelling Assumptions and list of symbols used for modelling

Before proceeding to develop the thermodynamic equations for the indoor dynamics of the building, there are a few assumptions that have been for modelling each of the dynamics. These are detailed here:

1. The air in the room is perfectly mixed and the temperature, humidity and CO_2 values that would be measured represent the average of the whole room.
2. The heat conductivity of the wall and window, k_{wa} and k_{wd} are constant.
3. Under steady-state conditions, the heat transfer through the wall is only along one dimension.
4. The convection on both sides of the wall is equal to the conduction through the surface of the wall.
5. The exchange of air between the inlet, outlet and the room under steady state conditions is isobaric. In other words, the air mass in the room does not change over time.

6. Under steady state-conditions, diffusion of water vapour through building components such as walls and windows is negligible compared to the change that is caused due to fresh air inlet.

7. There is no absorption of CO_2 from any of the elements in the room, including walls, windows and furniture.

For brevity, the list of symbols used in the following section are detailed in Table 2-1.

Table 2-1: List of symbols used for thermodynamical modelling

Symbol	**Description**
T	Temperature
u	mass flow rate of fresh air (kg/s)
c	Specific heat capacity (kJ/kgK)
ρ	Density (kg/m^3)
V	Volume (m^3)
h	Heat transfer coefficient $(W/m^2.K)$
A	Area (m^2)
q	Thermal load
C_p	Thermal Mass of the room(J/K)
R	Thermal resistance (K/W)
Subscripts	**Description**
wd	window
wa	wall
rm	room
s	supply air
a	air
w	water
i	Index for room number

2-2 Principles of building thermal modelling

Thermal Mass or Thermal Capacitance In building terminology, thermal mass is known as the property of the mass of a given building which allows it to store heat, thereby preventing the building from experiencing huge temperature fluctuations. This is analogous to be behavior of a capacitor in an electrical circuit. It is typically measured in units of J/K. The thermal mass of a body is given by the equation

$$C_p = \rho V c$$

where, ρ represents the density of the body, V represents the volume occupied by the body and c is the specific heat capacity of the material.

Thermal Resistance Thermal resistance is a heat property and a measurement of a temperature difference by which an object or material resists a heat flow. It is typically measured in

units of K/W. This is analogous to the behaviour of a resistor in an electrical circuit. The analog of the heat flow, q is current, and the analog of the temperature difference, $T_1 - T_2$, is voltage difference. With this complete thermal-electrical analogy, Thermal resistance R can be defined as ,

$$R = \frac{T_1 - T_2}{q}$$

This is equivalent to the result that is derived using Fourier's Law of Heat Conduction, where,

$$R_{cond} = \frac{L}{kA}$$

where L is the length of the material, k is the thermal conductivity of the material and A is the cross sectional area perpendicular to the direction of heat flow and R_{cond} is the resistance due to conduction.

This concept of analogy of thermal resistance for conductance can also be extended to heat convection at a surface through Newton's law of cooling, which states that:

$$q = hA(T_s - T_\infty)$$

With the analogy to thermal potential modelling, the thermal resistance due to convection can be defined as,

$$R_{conv} = \frac{T_s - T_\infty}{q} = \frac{1}{hA}$$

where h is the heat transfer coefficient.

2-2-1 Thermal modelling applied to simplified wall

A typical heat transfer profile from the external environment to a room consists of both convection and conduction as indicated in the Figure 2-1. As the thermal resistances are in series, the total resistance,R_{tot} can be expressed as,

$$R_{tot} = \frac{1}{h_1 A} + \frac{1}{h_2 A} + \frac{L}{kA} \tag{2-1}$$

The heat transfer due to convection in medium 1 is given by the equation,

$$q_x = T_{\infty,1} - T_{s,1}(h_1 A)$$

Similarly, heat transfer in medium 2 is given by,

$$q_x = T_{s,2} - T_{\infty,2}(h_2 A)$$

and heat conduction due to the wall surface is,

$$q_x = \frac{kA}{L}(T_{s,1} - T_{s,2})$$

Using the above results and expressing heat transfer in terms of overall temperature difference and the total Thermal Resistance,R_{tot}, the expression can be obtained as:

$$q_x = \frac{T_{\infty,1} - T_{\infty,2}}{R_{tot}} \tag{2-2}$$

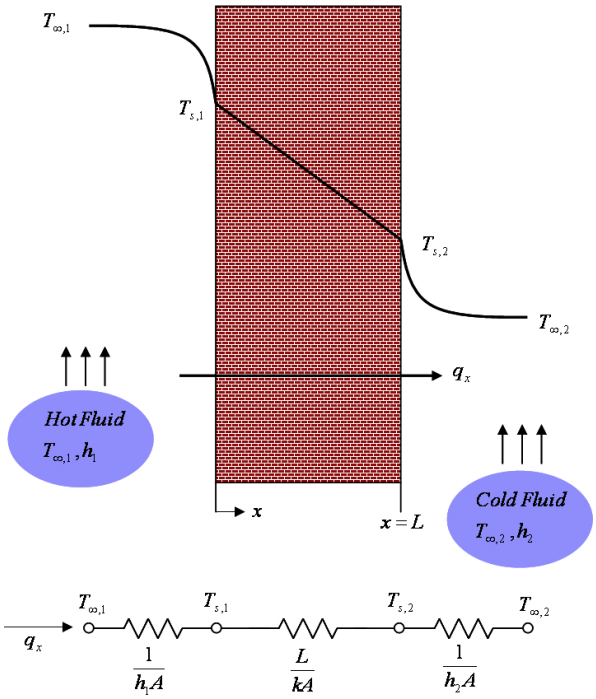

Figure 2-1: Heat transfer through a wall [4]

2-3 Modelling the temperature dynamics

Transmission and storage of heat constitute the heat dynamic properties of the building. The ability of a building element to store energy is proportional to its specific heat capacity. Apart from acting as a storage element, building walls and windows also act as a transmitter where they transfer heat between the room and the external environment. At the room level, the sources and sinks that affect the evolution of temperature in a room are quantified, as shown in Figure 2-2, the energy balance in steady state can be expressed as:

$$C_p \frac{dT_{rm_i}}{dt} = \underbrace{u_{rm_i} c_a (T_s - T_{rm_i})}_{\text{Cooling Load due to HVAC}} + \underbrace{h_{wa_i} A_{wa_i} (T_{wa_i} - T_{rm_i})}_{\text{Conduction through walls}} + \underbrace{h_{wd_i} A_{wd_i} (T_{wd_i} - T_{rm_i})}_{\text{Conduction through windows}} + \underbrace{q_{sol}}_{\text{solar radiation}} + \underbrace{q_{int}}_{\text{Occupants and Equipment}} \tag{2-3}$$

From equation 2-3, T_{wa} and T_{wd} constitute unmeasurable variables.

The temperature of these surfaces can be estimated by a combination of conductive and conductive heat transfer equations and can be expressed as:

$$T_{wa} = T_{rm} + \frac{T_{out} - T_{rm}}{R_{wa} A_{wa} h_{rm_1}} \tag{2-4}$$

where h_{rm_1} and h_{out_1} are the convective heat transfer coefficient of the inner wall and outer

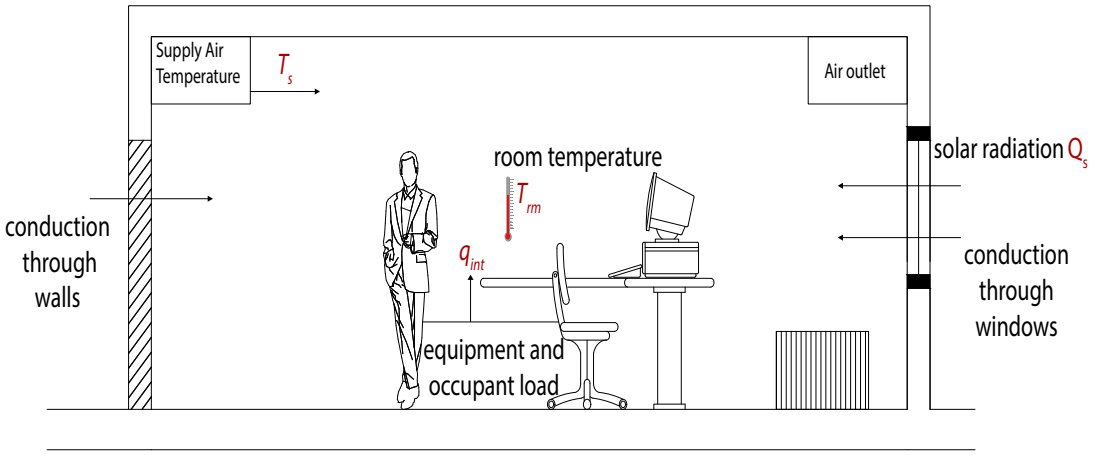

Figure 2-2: Schematic of Heat gains contributing to temperature change in a room

wall surface respectively and

$$R_{wa} = \frac{1}{h_{rm_1} A_{wa}} + \frac{l}{k_{wa} A_{wa}} + \frac{1}{h_{out_1} A_{wa}}$$

Similarly the window temperature T_{wd} can be expressed as,

$$T_{wd} = T_{rm} + \frac{T_{out} - T_{rm}}{R_{wd} A_{wd} h_{wd}} \tag{2-5}$$

where h_{rm_2} and h_{out_2} are the convective heat transfer coefficient of the inner window and outer window surface respectively and

$$R_{wd} = \frac{1}{h_{rm_2} A_{wd}} + \frac{l}{k_{wd} A_{wd}} + \frac{1}{h_{out_2} A_{wd}}$$

Now that these unmeasurable variables have been defined, Equation 2-3 now reads as,

$$\frac{dT_{rm}}{dt} = K_1 T_{rm} + K_2 T_s + K_3 T_{out} + K_4 (q_{sol} + q_{int}) \tag{2-6}$$

where,

$$K_1 = \frac{-1}{\left(\frac{u_{rm_i} c_a}{C_p} + \frac{1}{R_w a C_p} + \frac{R_w d}{C_p} \right)} \qquad K_2 = \frac{u_{rm_i} c_a}{C_p}$$

$$K_3 = \frac{1}{R_w a C_p} + \frac{1}{R_w d C_p} \qquad K_4 = \frac{1}{C_p}$$

From 2-6, it can be seen that the term K_1 contains the control control input is multiplied by the state which results in the formation of a bilinear system. This continuous-time bilinear

model is discretized with $\Delta t = 10$ min using a Backward Euler approach, which is well suited for systems with low sampling rates, such as HVAC systems [30]. For the testbed available in 3mE, it was not possible to obtain supply air flow rate values. Therefore, it is proposed to 'hide' this input air flow rate term into the constant K_1. Once K_1 is computed and the states are known, u_{rm_i} can be derived using a simple inversion, under the conditions [31]:

$$u_{rm_i}^{min}(k)(T_s(k) - T_{rm_i}(k)) \leq K_1(T_s(k) - T_{rm_i}(k)) \leq u_{rm_i}^{max}(k)(T_s(k) - T_{rm_i}(k)) \tag{2-7}$$

With these simplifications, the discrete time model can be written as:

$$T_{rm}(k+1) - a_1 T_{rm}(k) = b_1 T_s(k+1) + b_2 T_{out}(k+1) + b_3(q_s(k+1) + q_{int}(k+1)) \tag{2-8}$$

where,

$$a_1 = \frac{1}{1 - \Delta t K_1} \qquad b_1 = \frac{\Delta t K_2}{1 - \Delta t K_1}$$
$$b_2 = \frac{\Delta t K_3}{1 - \Delta t K_1} \qquad b_3 = \frac{\Delta t K_4}{1 - \Delta t K_1}$$

2-4 Modelling of the CO_2 dynamics of the building

The CO_2 concentration in a room can be computed using 2 approaches; the first approach being a direct white box based model for the ideal condition where there is assumed to be no infiltration from neighbouring conditions and the second one is a system identification based approach assuming non-ideal conditions. Please note that unlike other sections in this report, in this section, the symbol C refers to CO_2 concentration and not thermal mass.

In the development of physics based HVAC system models, dynamic models are commonly utilized for the slow moving temperature and humidity processes (e.g., zone temperature dynamics and zone humidity dynamics), and static models are utilized for the fast moving dynamics and energy consumption (fan or pump energy consumption). However, there exists very few dynamic modelling strategies to model the CO_2 dynamics in a room. In this section, a simplified mass balance based equation is developed to compute the CO_2 dynamics within a room.

As was the strategy with the previous section, the sources for the change in CO_2 content in a room are outlined. The main source of CO_2 is through the fresh air from the VAV box. Another main source of CO_2 occupancy is through the respiration of the users present in the room. This is depicted in Figure 2-3.

Modelling CO_2 dynamics is challenging due to the inherent complexity of air dynamics. However, under the consideration that the CO_2 sensor is placed at the level of the head of a seated occupant, this could give a sufficiently good response of the dynamics of CO_2 centered around the user. This positioning is important to measure the exact CO_2 level at the user level since a warm breath from the occupant acts as a bubble of gas that rises to the ceiling. This is because CO_2 is more buoyant than cooler ambient air [5]. This internal difference in the CO_2 levels within a room is highlighted in Figure 2-4.

With these considerations, under normal HVAC operation the CO_2 evolution can be described as,

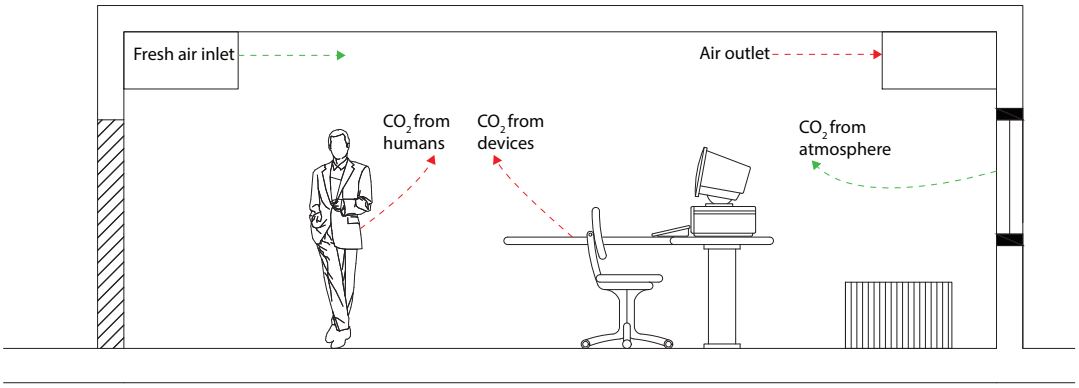

Figure 2-3: Schematic of sources and sinks for CO_2 in an office room

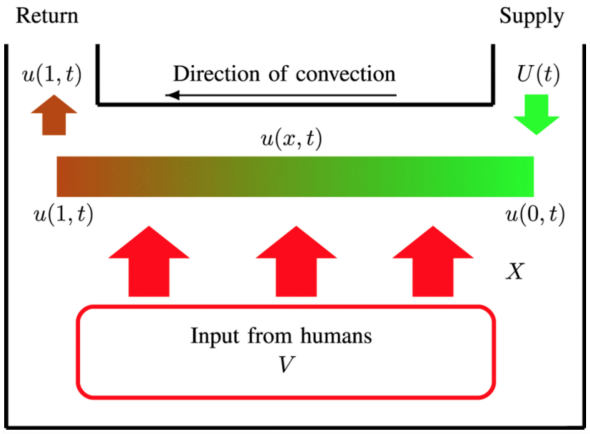

Figure 2-4: Evolution of CO_2 within a room [5]

$$\frac{dC_{rm}}{dt} = \underbrace{u_{rm_i}(C_s - C_{rm})}_{\text{due to ventilation}} + \underbrace{C_{occ}}_{\text{occupants}} + \underbrace{u_{out}(C_{out} - C_{rm})}_{\text{window infiltration}} + \underbrace{e}_{\text{infiltration from nearby zones}} \tag{2-9}$$

where C_{rm} is the CO_2 concentration in the room, C_s is the CO_2 concentration of inlet air, C_{out} is the CO_2 concentration of outside air, u_{out} is the mass flow rate of outside air into the room, e accounts for infilitration through nearby zones, and C_{occ} is CO_2 generated by occupants of the room. A simplified equation for CO_2 generated by occupants is given as:

$$C_{occ}(t) = n(t)C_n(t)$$

with $n(t)$ as the number of occupants at a given time instant and C_n as the exhalation rate per occupant.

2-4-1 White box modelling of CO_2 dynamics

In this section, a fixed amount of CO_2 exhalation of each occupant is assumed, considering standard office conditions. The primary factors which affect the rate of CO_2 generation by an average human are dependent on size, diet, level of physical activity. According to [32], the average rate of an occupant CO_2 perspiration can be estimated by first estimating the average oxygen consumption V_{O_2}.

This is done by:

$$V_{O_2} = \frac{0.00276 A_d M}{0.23RQ + 0.77}$$

where A_d is DuBois surface area, M is the metabolic rate per unit of surface area, and RQ is the respiratory quotient. Once this is obtained, the relationship between CO_2 generation rate and O_2 consumption rate is given by:

$$C_n = RQ.V_{O_2} \tag{2-10}$$

Based on this information, the average CO_2 generation rate corresponding to an average adult can be estimated, with $A_d = 1.8m^2$, engaged on light activity in an indoor office environment, with $M = 69.78W/m^2$ and average respiratory quotient of 0.83, thereby generating an CO_2 at the rate of $0.0052L/s$ ($0.0052kg/s$). This simplifies the model procedure since the volume of the room is fixed and using occupancy sensors, the amount of CO_2 generated per person can be determined and the model described in 2-11 can be obtained.

$$\frac{dC_{rm}}{dt} = \underbrace{u_{rm_i}(C_s - C_{rm})}_{\text{due to ventilation}} + \underbrace{0.0052n}_{\text{occupants}} \tag{2-11}$$

2-4-2 Greybox modelling of CO_2 dynamics and occupancy estimation

The modelling technique in this section is motivated by the work done in [24]. The whitebox model in the previous section generate models of sufficient accuracy. This approach, however, does come with a few limitations since the metabolic rates and physical characteristics are generalized. This approach also assumes that the occupancy status is always known, which might not always be the case in most buildings. Therefore, this work also incorporates a greybox modelling structure to estimate the dynamics of CO_2 evolution and also estimate occupancy status based on this measurements.

To formulate a linear model suitable for system identification, Equation 2-9 is discretized using Implicit Euler method to obtain:

$$C_{rm}(k+1) = C_{rm}(k) + \Delta t\Big(u_{rm_i}(C_s(k+1) - C_{rm}(k+1)) + N(k+1)C_n + u_{out}(C_{out}(k+1) - C_{rm}(k+1)) + e(k+1)\Big)$$

Simplifying this expression, the discrete time dynamics for CO_2 in a room is given by:

$$C_{rm}(k+1) = G_1 C_{rm}(k) + G_2 C_s(k+1) + G_3 C_{out}(k+1) + G_4 n(k+1) + G_5 e(k+1) \tag{2-12}$$

where,

$$G_1 = \frac{1}{1 + \Delta t(u_{rm_i} + u_{out})} \qquad G_2 = \frac{\Delta t u_{rm_i}}{1 + \Delta t(u_{rm_i} + u_{out})}$$
$$G_3 = \frac{\Delta t u_{out}}{1 + \Delta t(u_{rm_i} + u_{out})} \qquad G_4 = \frac{\Delta t C_n}{1 + \Delta t(u_{rm_i} + u_{out})}$$
$$G_5 = \frac{\Delta t}{1 + \Delta t(u_{rm_i} + u_{out})}$$

The model described in Equation 2-12 can be estimated using a suitable identification technique such as Prediction Error Method (PEM) or Maximum Likelihood Estimation (MLE). With the identified model, a simple inversion can be performed on Equation 2-12 to estimate the number of occupants n using the equation:

$$\lceil n(k+1) \rceil \approx \frac{C_{rm}(k+1) - G_1 C_{rm}(k) - G_2 C_s(k+1) - G_3 C_{out}(k+1) - G_5 e(k)}{G_4} \tag{2-13}$$

With this framework for occupancy estimation, it is possible to design a framework for Demand Controlled Ventilation (DCV) so that the cooling/heating strategy of the room can be decided based on the occupancy status of the room.

2-5 Modelling of the humidity dynamics of the building

As with the modelling strategy for temperature and CO_2, the strategy can be duplicated to modelling the humidity dynamics of the room as well. The internal sources for the rate of change in humidity are the Cooling and Heating air from the Variable Air Volume (VAV) box of the HVAC and moisture generated from humans and devices present in the room. The external sources are outside air and air from corridor and adjacent rooms.

As in the previous section, mass balance equations are used to obtain the model for Humidity as shown in 2-14:

$$\frac{dH_{rm}}{dt} = u_{rm}(H_s - H_{rm}) + u_{out}(H_{out} - H_{rm}) + \delta H_d \tag{2-14}$$

where where H_{rm} is the humidity in the room, H_s is the humidity of inlet air, H_{out} is the humidity of outside air and δ_{H_d} is modelled as a disturbance which can be attributed secondary sources of moisture such as water supplies, infiltration from neighbouring zones present in the room and human respiration.

Post discretization, the humidity dynamics of the room can be written as:

$$H_{rm}(k+1) = K_1 H_{rm}(k) + K_2 H_s(k+1) + K_3 H_{out}(k+1) + K_4 \delta H_d(n+1) \tag{2-15}$$

where,

$$K_1 = \frac{1}{1 + \Delta t(u_{rm} + u_{out})} \qquad K_2 = \frac{\Delta t u_{rm}}{1 + \Delta t(u_{rm} + u_{out})}$$
$$K_3 = \frac{\Delta t u_{out}}{1 + \Delta t(u_{rm} + u_{out})} \qquad K_4 = \frac{1}{1 + \Delta t(u_{rm} + u_{out})}$$

2-6 Summary

Strategies capable of estimating the dynamics of the room temperature, humidity, CO_2 and occupancy estimation have been constructed in this chapter. Reformulating the system dynamics in a regression format has allowed the use of well defined system identification tools, with potential for realizing accurate models. Decoupling of these dynamics has also ensured that these variables can be controlled individually.

Chapter 3

Identification and validation of dynamic models

This section deals with the experiments to identify and validate the proposed models. Section 3-1 deals with the description of the model structure and Identification methods that can potentially be used for the graybox identification. Section 3-3 discusses some of the results achieved during the experimental validation and comparison with standard identification methods.

3-1 Model structure and Identification methods

To realize the objectives proposed in Chapter 2, it is imperative that a suitable model structure be chosen, in such a way that this structure is flexible enough to incorporate both deterministic dynamics and stochastic dynamics. Available methods and techniques that are currently in use will be discussed in this section.

One of the most common methods to describe a discrete system is by using the Linear Polynomial model. This is generally represented by the equation:

$$y(k) = G(z,\theta)u(k) + H(z,\theta)e(k) \tag{3-1}$$

Where $u(k)$ and $y(k)$ are the inputs and outputs of the system respectively and $e(k)$ is the disturbance (modelled as a zero mean, white noise). $G(z,\theta)$ and $H(z,\theta)$ represent the transfer functions of the deterministic and stochastic parts of the system respectively. z^{-1} represents a backward shift operator, that is, it defines the number of the delay samples between the input and the output signals.

Furthermore, we can define the transfer functions G and H as:

$$G(z,\theta) = \frac{B(z,\theta)}{A(z,\theta)F(z,\theta)} \tag{3-2}$$

$$H(z,\theta) = \frac{C(z,\theta)}{A(z,\theta)D(z,\theta)} \tag{3-3}$$

Here, the vector θ is the set of parameters that need to be identified. Thus, writing the system in a more general form, we can express it as,

$$A(z)y(k) = \frac{B(z)}{F(z)}u(k-n) + \frac{C(z)}{D(z)}e(k) \tag{3-4}$$

Using this general polynomial equation and setting one or more of $A(z)$, $C(z)$, $D(z)$ and $F(z)$ to 1, we obtain well known model structures such as ARX (Autoregressive with exogenous terms), ARMAX (Autoregressive Moving Average with exogenous terms), Box-Jenkins model and output error models.

3-1-1 ARMAX Models

Thus, the equation reduces to:

$$A(z)y(k) = B(z)u(k-n) + C(z)e(k) \tag{3-5}$$

The regression involves finding the co-efficients A(z), B(z) and C(z), such that the residual error $e(k)$ contains only a Gaussian white noise of minimal variance σ_e^2. Traditionally, ARMAX based model have always fallen into the category of Black box modelling techniques. Since we have already framed the dynamics of the systems developed in Equations 2-8,2-12 and 2-15 in the format given in 3-5 with $n = 1$, this system is suitable for ARMAX identification.

To ensure that the model is estimated correctly, we identify the parameters using PEM. For a linear model given in the form 3-4, PEM uses a numerical optimization to minimize the cost function, a weighted norm of the prediction error, defined as follows for scalar outputs. The one-step prediction $\hat{y}[k|k-1]$ and prediction error are given as:

$$\hat{y}[k|k-1] = \sum_{j=0}^{\infty} \tilde{g}(n)u(k-n) + \sum_{j=1}^{\infty} \tilde{h}(n)y(k-n)$$

$$\epsilon[k|k-1] = y(k) - \hat{y}(k|k-1) = H^{-1}(z)(y(k) - G(z)u(k))$$

Identification problem

Given $Z_n = y(k), u(k)]_{k=0}^{N-1}$, identify the values of the polynomials (A, B, C, D, F) and variance σ_e^2.

3-2 Experimental Setup

Experiments to evaluate the proposed models were done in a test-bed setup in Rooms I, K and M of the Faculty of Mechanical, Maritime and Materials engineering in TU Delft Campus. Table 3-1 enlists the physical characteristics of each of the rooms that were evaluated. All physical dimensions for the testbed were either obtained manually or with consultation from facility management. A floor plan with the rooms used for system identification is given in Figure 3-1.

Table 3-1: Physical characteristics of the room

Room Name	Volume (m^3)	Window Area (m^2)
I	396	65
K	360	57
M	396	65

All data for the simulations were obtained from the building management system provided by Johnson Controls, with a sample interface shown in Figure 1-6. The building is equipped with a VAV based HVAC system, where each VAV box controls the zone temperature individually. Temperature sensors are located on the ceiling of the room, and there are individual sensors placed in the AHU from where measurements are sampled. Data was measured from April 5 for a period of 4 weeks and sampled at a fixed rate of 10 minutes from the rooms. The outside temperature and solar radiation was retrieved from a weather station in the TU Delft campus.

From 2-8, we can easily deduce that the dynamics of system has a MISO ARMAX structure. For the validation of the experiments, we shall consider two scenarios to validate the identified models. This is because the model developed 2-8 does not considered the effect of neighbouring room since it was initially developed keeping a concrete wall in mind. In that case, due to extremely high thermal mass, it was considered that the effect of the neighbouring zones would not significantly affect the room temperature. However, since the 3mE testbed consists of partition walls with no concrete in between, it is believed that the thermal resistance is significantly higher thereby the room temperature would be far more sensitive to nearby temperature changes. The list of inputs and outputs considered for each of the scenarios are described in Table 3-2.

- Case 1: Considering the temperature of neighbouring room as an input to the model (high thermal mass of walls)
- Case 2: Ignoring the effects of the temperature of the neighbouring room (low thermal mass of walls) For this case, the thermodynamical equation describing heat transfer

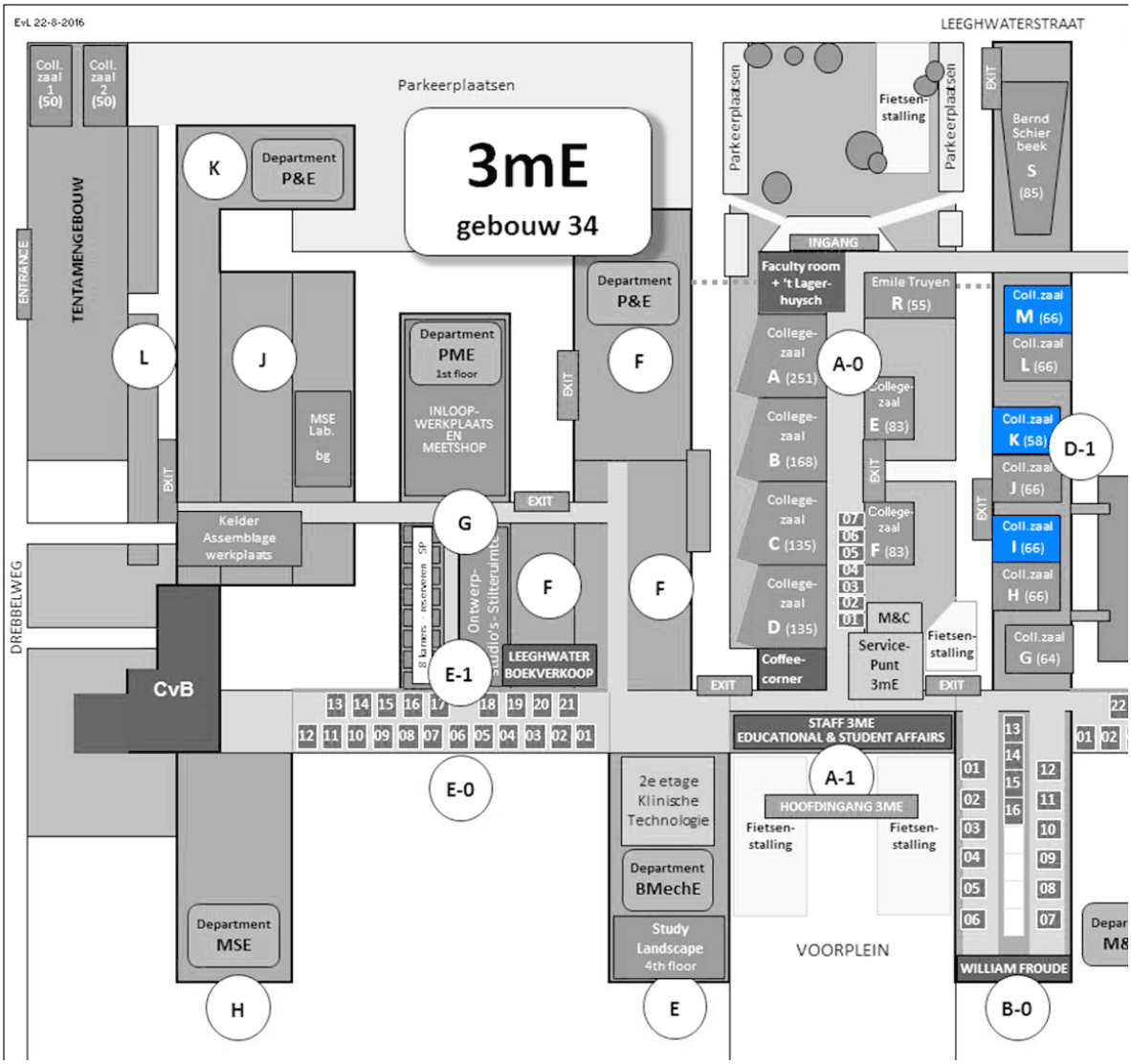

Figure 3-1: Floor plan of building with rooms used for identification highlighted in blue

is a slight modification of the original equation given in Equation 2-8. The modified equation incorporating heat transfer due to neighbouring zone is given as:

$$C_p \frac{dT_{rm_i}}{dt} = \underbrace{u_{rm_i} c_a (T_s - T_{rm_i})}_{\text{Cooling Load due to HVAC}} + \underbrace{R_{wa_o}(T_{out_i} - T_{rm_i})}_{\text{Conduction through building walls/windows}} +$$

$$\underbrace{R_{wa_j}(T_j - T_{rm_i})}_{\text{Conduction through neighbouring zone}} + \underbrace{q_{sol}}_{\text{solar radiation}} + \underbrace{q_{int}}_{\text{Occupants and Equipment}} \tag{3-6}$$

where T_j is the temperature of the neighbouring zone, R_{wa_o} is combined the thermal resistance of the wall and window facing the outside and R_{wa_j} is the thermal resistance

of the wall facing the neighbouring zone.

The discretized form of this can be written as:

$$T_{rm}(k+1) - a_1 T_{rm}(k) = b_1 T_s(k+1) + b_2 T_{out}(k+1) + b_3 T_j(k+1) + b_4(q_s(k+1) + q_{int}(k+1)) \tag{3-7}$$

$$a_1 = \frac{1}{1 + \Delta t(\frac{u_{rm_i} c_a}{C_p} + \frac{1}{R_{wa_o}} + \frac{1}{R_j C_p})} \qquad b_1 = \frac{\Delta t u_{rm_i} c_a}{C_p\left(1 + \Delta t(\frac{u_{rm_i} c_a}{C_p} + \frac{1}{R_{wa_o} C_p} + \frac{1}{R_j C_p})\right)}$$

$$b_2 = \frac{1}{R_{wa_o} C_p\left(1 + \Delta t(\frac{u_{rm_i} c_a}{C_p} + \frac{1}{R_{wa_o} C_p} + \frac{1}{R_j C_p})\right)}$$

$$b_3 = \frac{1}{R_j C_p\left(1 + \Delta t(\frac{u_{rm_i} c_a}{C_p} + \frac{1}{R_{wa_o} C_p} + \frac{1}{R_j C_p})\right)}$$

$$b_4 = \frac{1}{C_p\left(1 + \Delta t(\frac{u_{rm_i} c_a}{C_p} + \frac{1}{R_{wa_o}} + \frac{1}{R_j C_p})\right)}$$

Table 3-2: Inputs and outputs for case based scenarios

Scenario	Inputs	Outputs
Case 1	T_{out}, T_s, q_{sol}	T_{rm}
Case 2	T_{out}, T_s, T_j, q_{sol}	T_{rm}

The obtained data was generally unfit for estimation due to missing samples in a few intervals and mismatch of timestamps. These were therefore pre-processed using interpolation and data resampling to ensure all data had the same timestamps. Using the above datasets, a series of simulations was run on MATLAB to determine the validity of the structure, the number of data points required for a good fit and also improvements over the obtained model. Figure 3-2 shows the temperature input variables that were used for identification process and the 3-3 shows the solar irradiance values that were used.

The results from Figures 3-4 and 3-5 compare these 2 models. It confirms our suspicion that the the room temperature of the neighbouring zones (corridor and neighbouring classrooms in this case) significantly affect the temperature of the modelled zone. Therefore, for the rest of this chapter, the models with heat transfer due to neighbouring walls included shall be considered.

3-3 Experimental results

Assuming that the parameterized model is suitably well defined, the k-step ahead prediction error, for a reasonable value of k is nothing but a white noise sequence. To simplify the

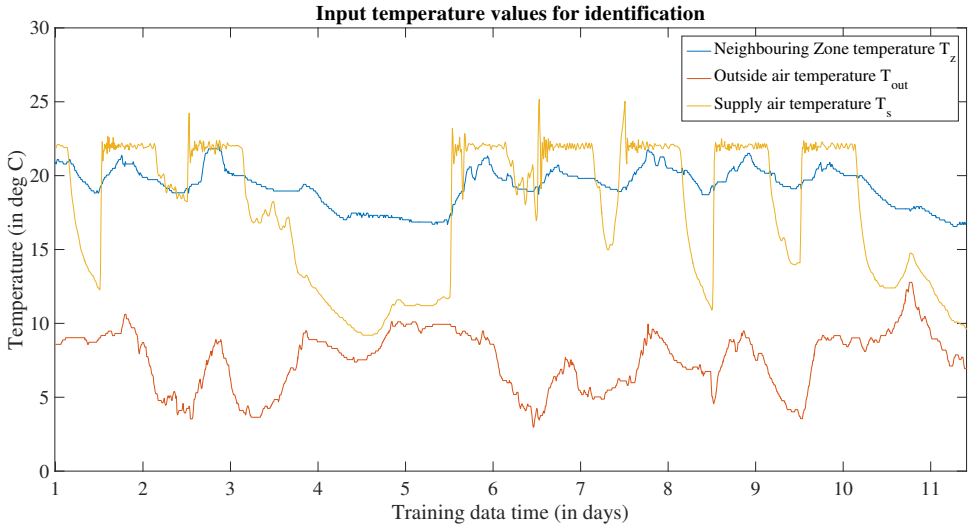

Figure 3-2: Input Temperature variables used for identification

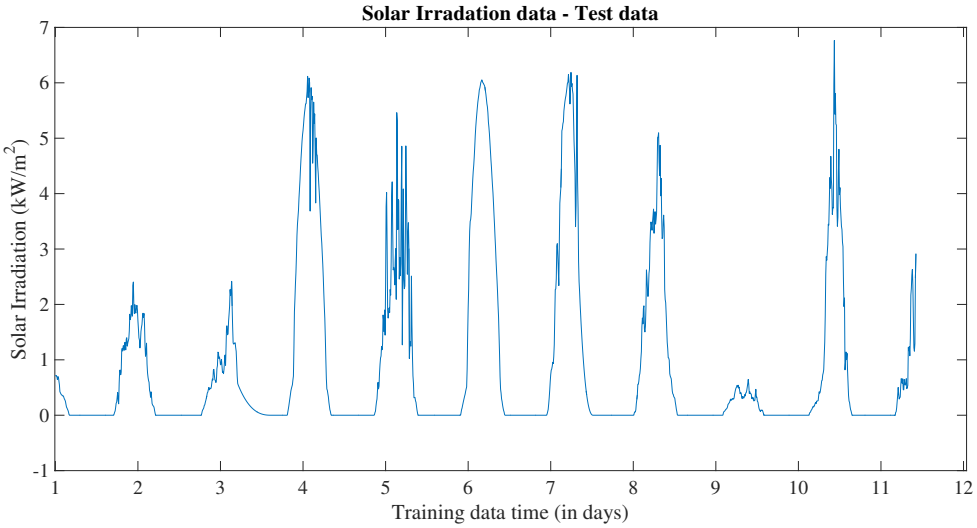

Figure 3-3: Solar Irradiance values used for identification

analysis, only ARX type models are considered (Equation 3-5 with C=A), to ensure that only the deterministic part of the equation are estimated. This also ensures that the prediction error is linear in parameters. To validate the model, 2 metrics to evaluate the accuracy of prediction are used: mean squared error (MSE) of predicted data and variance accounted for (VAF) of estimated data. These can be defined as:

$$\text{MSE} = \frac{1}{n}\sum_{i=1}^{n}(T_{rm_i} - T^*_{rm_i})^2$$

$$\text{VAF} = \left(1 - \frac{\text{var}(T_{rm_i} - \hat{T}_{rm_i})}{\text{var}(T_{rm_i})}\right) \cdot 100\%$$

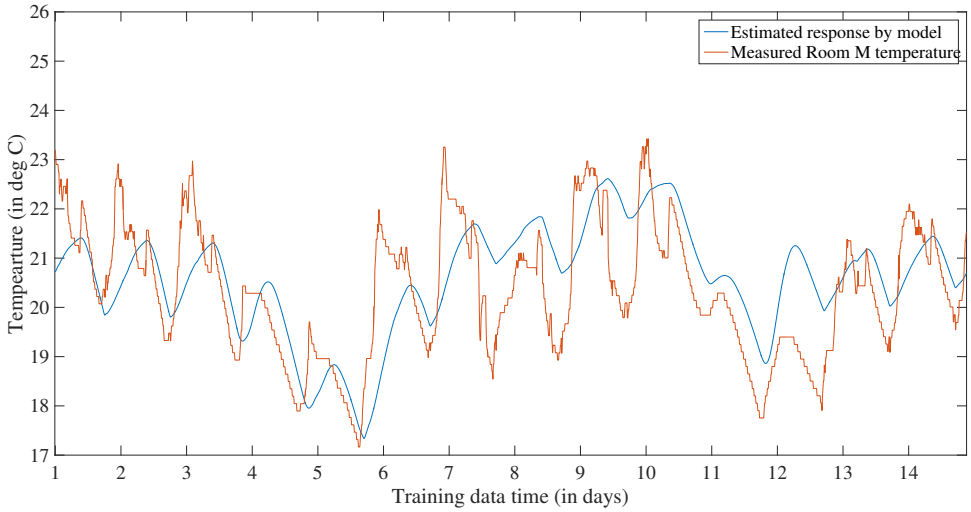

Figure 3-4: Model output for Case 1, T_j not considered as an input

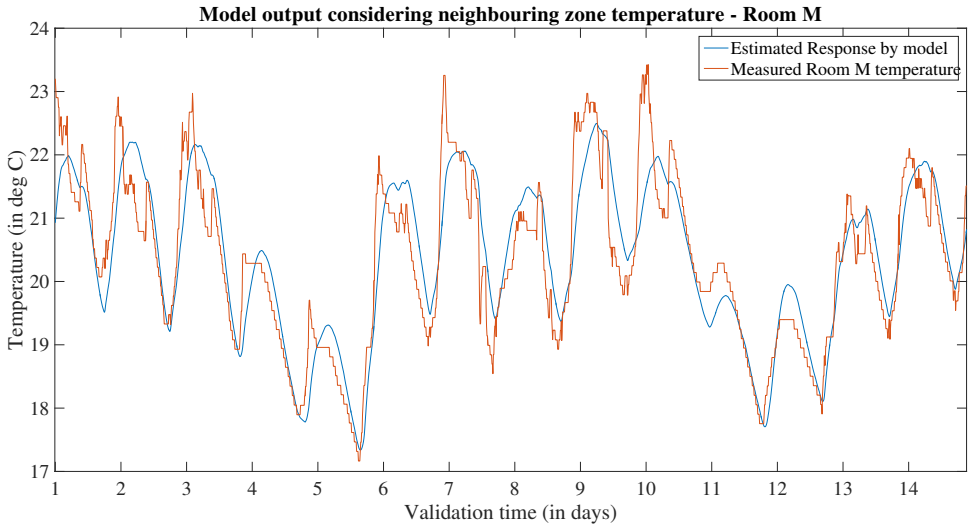

Figure 3-5: Model output for Case 2, T_j considered as an input

where T_{rm_i}, $T^*_{rm_i}$ and $\hat{T}_{rm_i}$ are the measured, predicted and estimated values of room temperature respectively and var denotes variance.

As a measure to select the minimum size of training data to ensure a good fit while also ensuring that the data is not overfitted. The VAF of model output is computed for a validation dataset was used of 2000 samples ($\approx$ 14 days). The training dataset size which corresponds to maximum VAFs is selected. An indicative plot showing the evolution of VAF with the training days for test case Room M is given in Figure 3-6.

From Figure 3-6 we notice that a good VAF after 1100 ($\approx$ 9 days) samples, peaking at $\approx 85\%$ around 1300 samples ($\approx$ 11 days). Figures 3-7 and 3-8 are 2 indicative plots which show the validation of the rest of the models that were considered for identification. In general,

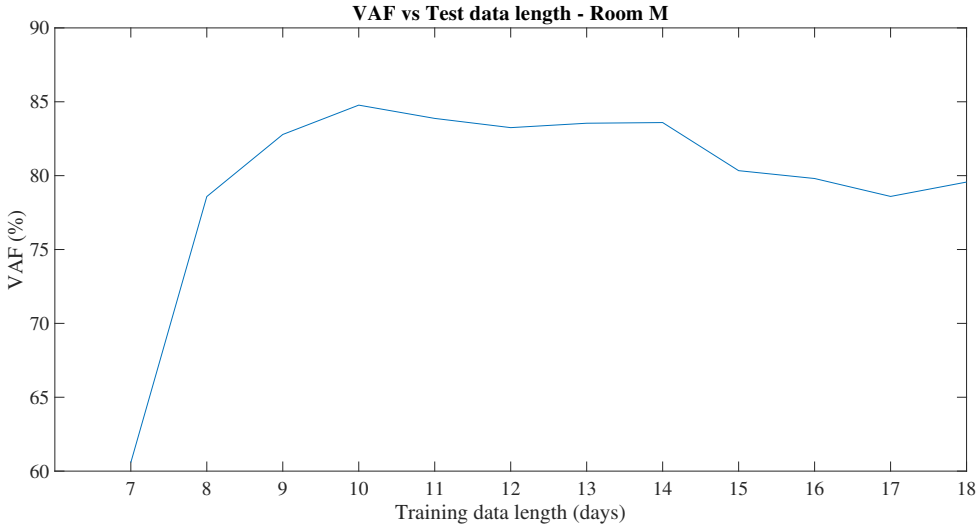

Figure 3-6: Evolution of VAF with training samples

the results of the identification indicate a good fit overall and the estimated model is able to capture the dynamics of the overall room.

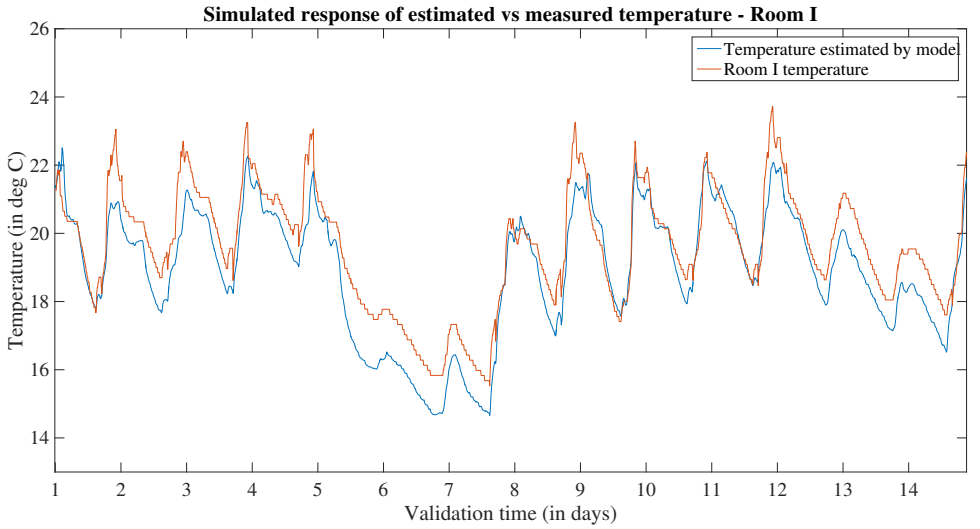

Figure 3-7: Comparison of Measured and Estimated Response - Room I

Table 3-5 summarizes the results of the identification problems along with validation parameters and length of validation and training data. The overall Variance Accounted For (VAF) varies between 69 and 83 percent, which indicates a reasonably good prediction of the model. Even during 'set-back' times, i.e. when temperature setpoints are lowered during night or in the weekend, the system tracks the model dynamics quite well. This is inspite of the presence of stochastic disturbances such as use of radiators (whose temperature could not be monitored), occasional opening of windows, infiltration through doors and heat generated internally through occupants, indicating the effectiveness of the discrete time system

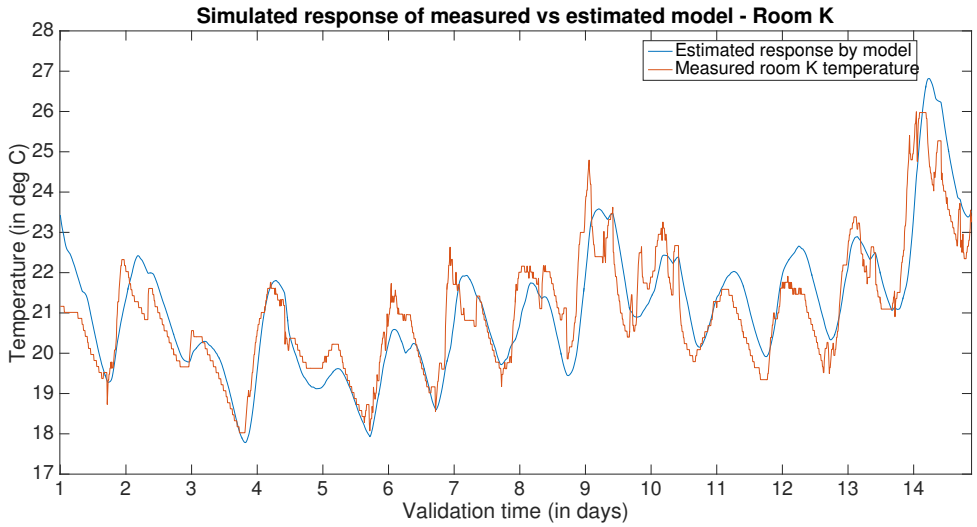

Figure 3-8: Comparison of Measured and Estimated - Room K

identification approach.

Table 3-3: Results obtained after System Identification

Room Name	MSE	VAF (%)
I	0.0083	80.27
K	0.0016	69.41
M	0.0090	83.24

The obtained coefficients from the system identification procedure for system given in Equation 2-8 are shown in Table 3-4. The high values of the identified parameter due to neighbouring zones, b_3, indicates that the neighbouring zones have a large impact on the temperature of the rooms. This means that these zones have very low thermal mass, thereby possessing poor thermal insulation and is easily susceptible to temperature fluctuations from outside.

Table 3-4: Identified parameters from Equation 3-7 for Individual rooms

Room	a_1	b_1	b_2	b_3	b_4
Room I	0.9627	-0.0043	0.005	0.033	0.001
Room K	0.9614	-0.0039	0.004	0.038	0.004
Room M	0.9512	-0.002	0.0073	0.043	0.0007

3-3-1 Comparison with blackbox models

To indicate the effectiveness of the greybox modelling technique, it was compared with a system identified using Multivariable Output Error State Space (MOESP), a well known Subspace system identification technique. Based on the Singular Value Decomposition plot

of the block Hankel matrices created for multiple orders, an order of 2 was chosen as the this was the least order with which the system could be described accurately.

As Figure 3-9 shows, the response of these systems is almost exactly the same, with the MOESP based model performing only marginally better. A comparison of model validation parameters is shown in Table 3-5. Various other techniques yielded similar results, thereby reaffirming our notion that the ARMAX based greybox model is suitable both in terms of system order and model fit. It can also be noted that the model identified through MOESP cannot be inverted to estimate the input mass air flow values, as described in 2-7.

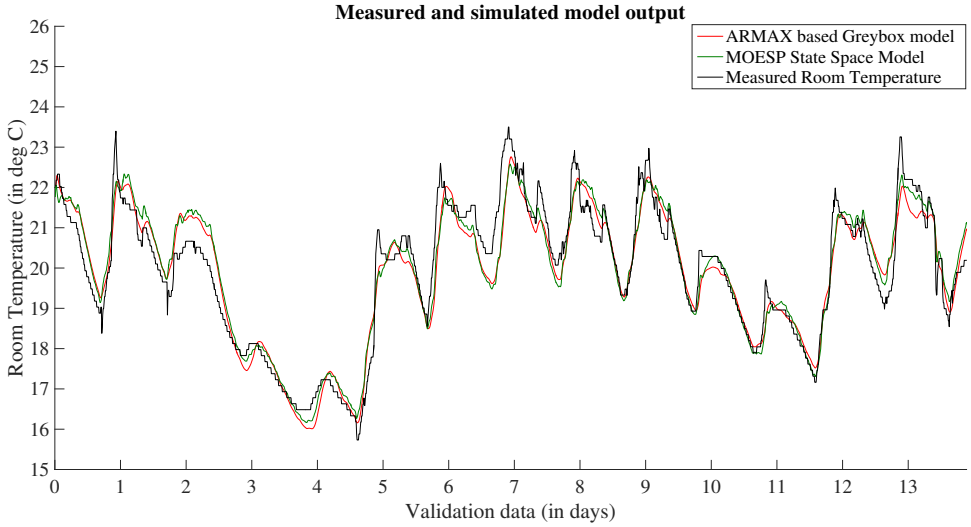

Figure 3-9: Comparison of Fit between Greybox and MOESP estimated blackbox model

Table 3-5: Comparison between Greybox ARMAX and MOESP Subspace Identification - room M

Method	System Order	MAE	MSE	VAF (%)
ARMAX	1	0.0692	0.0080	83.24
MOESP	2	0.0640	0.0076	88.48

3-4 Improvement of prediction results with a Kalman filter

The above model, however, is a simplified linear prediction of the dynamics of the system, and can only simulate the response of the system to a moderate degree. Further accurate predictions of the system would require the definition of additional states to the system, such as neighbouring wall temperatures, ceiling and floor temperature, and heat influx through other sources such as the corridor. However, this could lead to an high number of states, making it highly unsuitable for control design, considering that a typical building has a lot of rooms. Furthermore, these additional states also have complex relationships between them, leading us back to a nonlinear model.

To avoid this, a Kalman filter is used to estimate the time varying unknown internal loads.

The Kalman filter can effectively estimate unmeasurable states using knowledge of the system, while also accounting for measurement and system noise. It follows from theory that the Kalman filter is the optimal linear filter in cases where the model matches the real system and the entering noise is white. Since the ARMAX estimated model follows the dynamics of the system quite well, it can be said that in an ideal case, ignoring unmeasurable disturbances, the model would matches the dynamics of real system. Furthermore, it has been assumed that the estimate of the unmeasurable parameters as a white noise. If these assumptions are valid, the model must fit perfectly to the measured system. To verify we, we perform k-step ahead predictions of $k = 1$ (= 10 mins), 12 (= 2 hours) and 24 (= 4 hours).

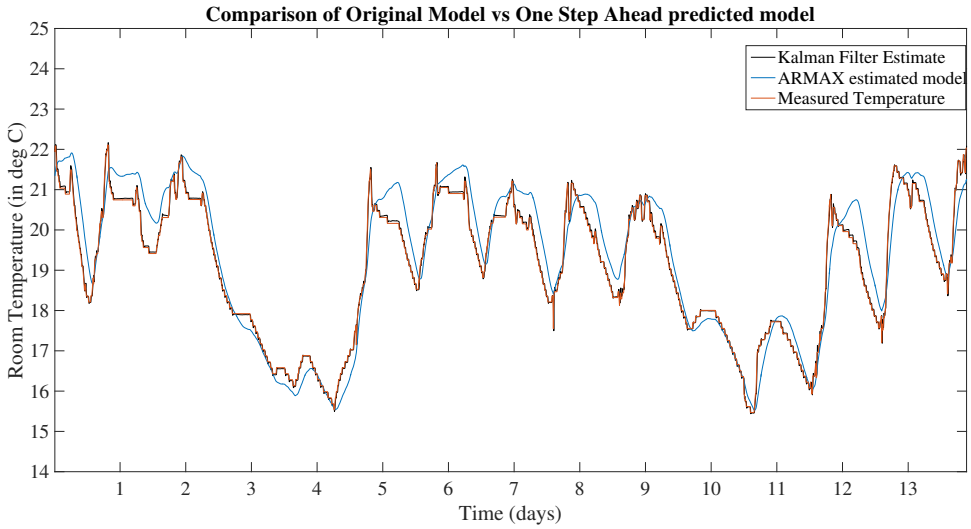

Figure 3-10: Comparison of Predicted, Estimated and Measured model

Figure 3-10 shows the output of the system for the a one-step ahead prediction horizon. Figure 3-11 shows the output of the system for $k = 12$ and $k = 24$. It is clear that even for prediction steps as large as 4 hours, the k-step ahead Kalman predictor can estimate the system very closely to the actual model. Therefore, it can be concluded that the ARMAX based modelling procedure gives very good and intuitive understanding of the temperature dynamics.

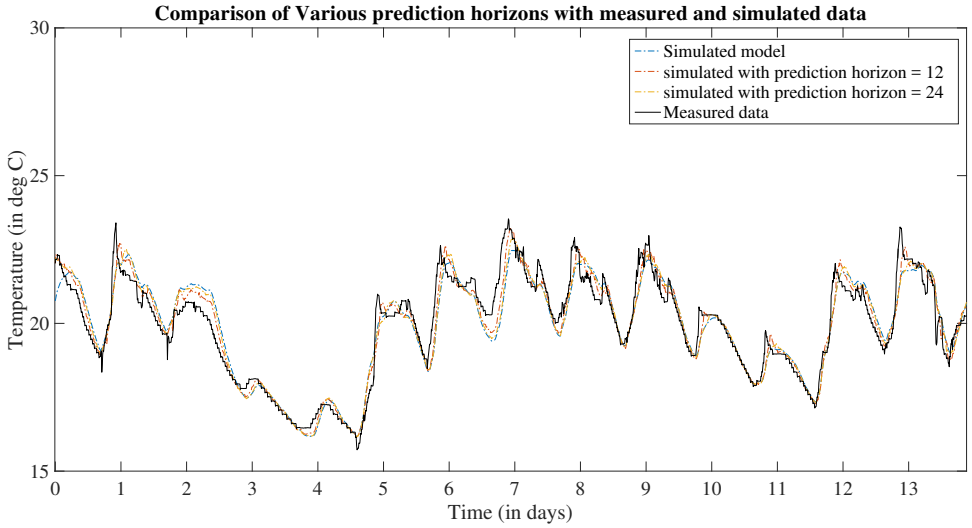

Figure 3-11: Comparison of Predicted, Estimated and Measured model for $k = 12$ and $k = 24$

3-5 Summary

In this chapter, the dynamical models developed in Chapter 2 were experimentally tested in the testbed for 3 sample rooms. The results indicate a good degree of fit with the experimental data validating the modelling methodology. It is important to note that the modelling strategy for CO_2 dynamics, occupancy estimation and Humidity were not validated experimentally due to unavailability of datasets. Therefore, further conclusions cannot be made about these dynamics. The next chapter gives a simulation based setup of an integrated control model that optimizes energy usage and comfort of the occupant.

Chapter 4

Strategies for improved control in office buildings

The previous sections dealt with the modelling and identification method for the temperature, humidity and CO_2 dynamics of a room. Using the developed model for these rooms, this section outlines the design of a supervisory control strategy. This control strategy involves an upper layer MPC which determines the setpoints for the room temperature and a lower level Proportional Integral (PI) control which controls individual rooms using these setpoints. This chapter is a proof-of-concept of how thermal comfort dynamics can be integrated into controller design.

4-1 Integrated modelling of HVAC dynamics

For this work, the focus will be on a cooling test case, as shown in Fig. 4-1, which models the dynamic interactions between 3 rooms and 1 corridor. Fig. 4-1 highlights the interacting structure of the HVAC system, with a Chiller that drives both a cooling coil of an AHU. The AHU is further connected to a VAV system which supplies fresh air into the rooms and the corridor. In this work, these controllers are minimizing the difference between the respective room temperature, T_{rm_i} and Room set-point temperature, T_{set}.

There are a few assumptions that are made while developing the above modelling framework:

1. The air and water in the subsystem units are well mixed and have the same temperature
2. There is no heat loss through ducts and pipes in the system
3. Thermal conductivity of wall is constant and the heat conduction through it is one-dimensional.

For brevity, the list of symbols used in the following section are detailed in Table 4-1.

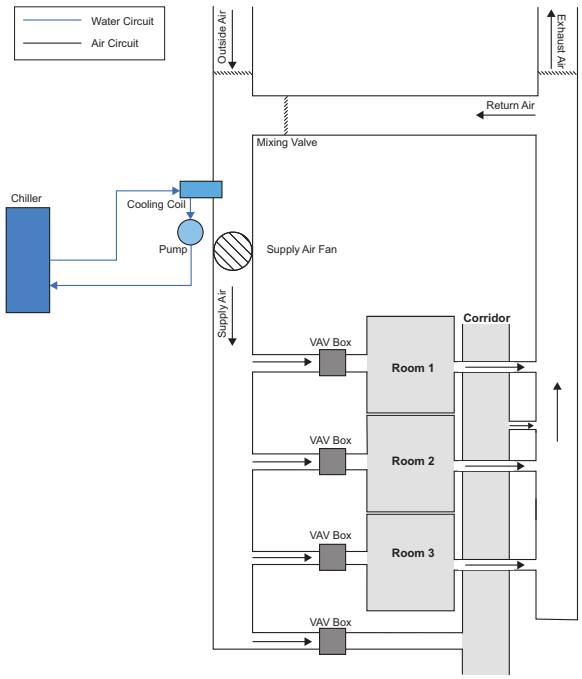

Figure 4-1: Schematic of the Test case HVAC System

Table 4-1: List of symbols used for integrated modelling

Symbol	**Description**
T	Temperature
u	control input (mass flow rate in kg/s)
c	Specific heat capacity (kJ/kgK)
ρ	Density (kg/m^3)
V	Volume (m^3)
A	Area (m^2)
U	Thermal transmittance of envelope (W/m^2K)
Q	Power (kW)
Subscripts	**Description**
out	outside air
rm	room
s	supply air
a	air
w	water
i	Index for room number
f	fan

For each of the rooms shown in the test case HVAC system shown in Figure 4-1, the simplified model for the room temperature dynamics is considered. A standard room made of concrete walls, gypsum boards and thick windows as construction materials is considered. These are fairly standard construction materials used in modern buildings. All of these considerations

were made with the properties of a typical office room in mind. The physical properties of these rooms are elaborated in Table 4-2.

Table 4-2: Physical parameters of the test case setup

Physical parameter	Room 1	Room 2	Room 3	Corridor
Area (m^2)	20	25	30	30
Height (m)	3	3	3	3
Thermal mass (kJ/K)	144	180	216	216
Thermal transmittance (kW/m^2K)	0.0110	0.0115	0.0120	0.0120

The equations describing the system with the physical parameters can be written in the following bilinear form :

$$[\text{Room}]\frac{dT_{rm}}{dt} = \frac{u_{rm}}{\rho_a V_{rm}}(T_s - T_{rm}) + \frac{U_e A_e}{c_a \rho_a V_{rm}}(T_{out} - T_{rm}) \tag{4-1}$$

The discretized (nonlinear) model for the room temperature is linearized around the point of $24°C$ for the room temperature since the temperature and input range is quite small and this is sufficient for our control purpose [4, 33]. The resulting discrete time LTI model can be represented using the standard state-space structure:

$$\begin{aligned} x(k+1) &= Ax(k) + Bu(k) \\ y(k) &= Cx(k) + Du(k) \end{aligned} \tag{4-2}$$

where $x = \begin{bmatrix} T_{rm_1} & T_{rm_2} & T_{rm_3} & T_{rm_4} \end{bmatrix}^T$ in $\mathbb{R}^4$ is the state, $u = \begin{bmatrix} u_{rm_1} & u_{rm_2} & u_{rm_3} & u_{rm_4} \end{bmatrix}^T$ in $\mathbb{R}^4$ is the input. For the sake of simplicity, the controller is designed ignoring disturbances. The numerical values of the state space matrix has been inserted in the Appendix.

4-2 Optimization problem formulation

The optimization involves: optimization of the low-level PI controls (in order to achieve acceptable tracking of the set points); optimization of the set-points (in order to minimize energy consumption and thermal discomfort). An intuitive schematic of the overall control strategy is represented in Fig. 4-2.

4-2-1 Optimization for low-level controllers

The four Proportional and Integral terms for the individual subsystem controllers (in the four VAV boxes) are generated through an offline optimization to track the desired set points while minimizing energy consumption of fan and pumps. With a common duct distributing airflow to all 3 rooms and the corridor, the total mass airflow that is blown by the fan is the sum of the individual inlet airflow rates in each room. Therefore, the equation for energy consumption by the fan is given as:

$$Q_f = \frac{\Delta P u_a}{1.0 \times 10^3} \tag{4-3}$$

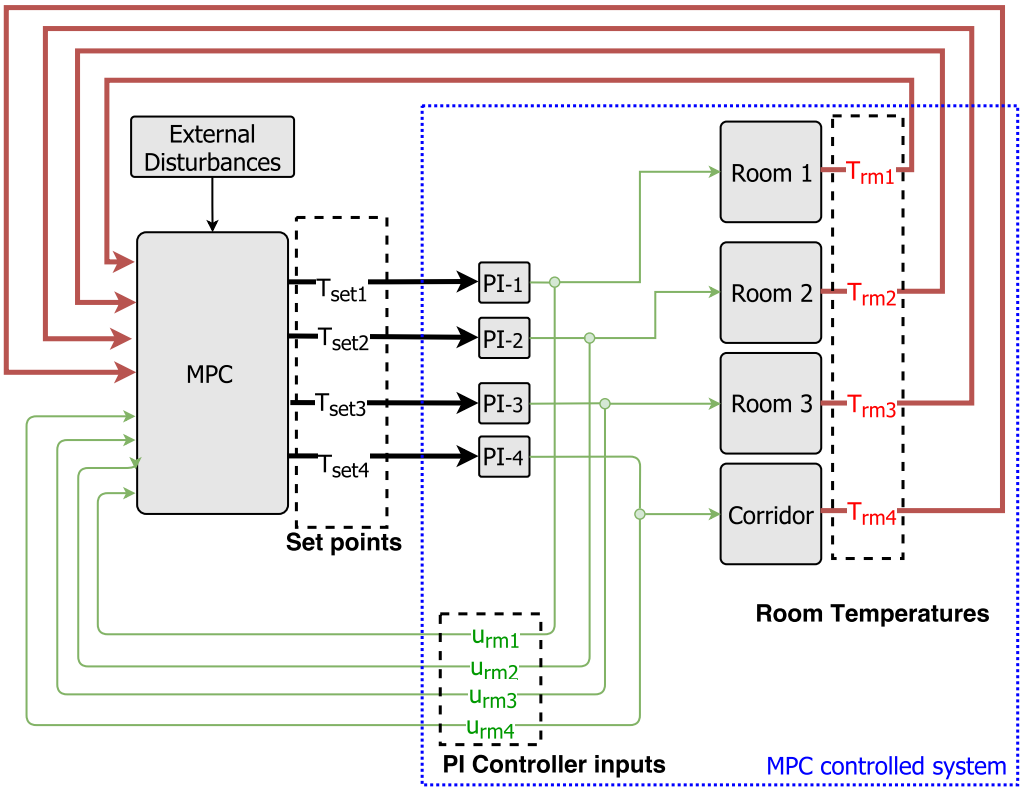

Figure 4-2: Schematic of proposed control strategy

where $u_a(k) = u_{rm_1}(k) + u_{rm_2}(k) + u_{rm_3}(k) + u_{rm_4}(k)$ is the sum of inlet flow rates of all the 4 rooms at any given time instant. The four controllers are optimized in a simulation-based fashion, with the command 'fmincon', to minimize the following multi-objective function

$$J = \sum_{k=1}^{\tau_f} \left(\sum_{i=1}^{4} (T_{rm_i}(k) - T_{set}(k))^2 \right) + 10^{-2}(Q_f^2)$$

where T_{set} is the desired zone temperature and τ_f represents the total duration of the simulation (in this case, 24 hours). The weight was chosen as 10^{-2} as a trade-off between good tracking and reasonable energy consumption. The number of optimization parameters are eight (four proportional and four integral gains). The optimal PI gains for each of the rooms are given in Table 4-3.

Table 4-3: Autotuned PI parameters computed through optimization

Gain	Room 1	Room 2	Room 3	Corridor
K_p	0.15	0.13	0.11	0.11
K_i	2×10^{-4}	1.8×10^{-4}	1.8×10^{-4}	1.8×10^{-4}

4-2-2 Optimization for set-point control

Thermal comfort quantification

The sense of thermal comfort of a human is a highly subjective sensation which could be attributed to various factors such as general health, geographical upbringing and general physical composition. Fanger proposed to quantify such factors and created a predictive model for whole body thermal comfort via the PMV index [34]. The PMV index is now standardized in the American Society of Heating, Refrigerating and Air-Conditioning Engineers (ASHRAE) thermal sensation scale [26]: this thermal scale runs from Cold (-3) to Hot (+3) where 0 indicates maximum user comfort. The equation for PMV index is

$$PMV = [0.303e^{-0.036M} + 0.028]L \tag{4-4}$$

where L is the thermal load, defined as the difference of metabolic heat generation and the calculated heat loss from the body to the actual environmental conditions, assuming optimal comfort conditions:

$$\begin{aligned} L = {} & M - W - 3.96 \times 10^{-8} f_{cl}[(t_{cl}+273)^4 - (t_r+273)^4] \\ & - f_{cl}h_c(t_{cl} - T_{rm}) - 3.05[5.73 - 0.007(M-W) - \rho_a] \\ & + 0.42[(M-W) - 58.15] - 0.0173M(5.87 - \rho_a) \\ & - 0.0014M(34 - T_{rm}) \end{aligned} \tag{4-5}$$

where f_{cl} is the clothing factor, h_c is the convective heat transfer coefficient, M is the metabolic rate $[W/m^2]$, ρ_a is the vapor pressure $[kPa]$, t_{rm} is the room air temperature, t_{cl} is the temperature of the clothing surface $[°C]$, t_r is the mean radiant temperature $[°C]$, W is the external work (taken as 0 for normal office conditions).

The mean radiant temperature is a difficult quantity to measure, since it involves measurement of the wall envelope and window temperature [35]. It is also a highly nonlinear function, which can be computationally expensive when included in the cost of the optimization. To overcome this, Rohles [36] proposed an adapted model of the PMV which expresses the thermal sensation as a function of parameters easily sampled in an office environment, such as air temperature and relative humidity. The boundary conditions of the modified PMV index were: clothing insulation level $I_{cl} = 0.6clo$, metabolic rate $M = 70W/m^2$, air velocity $v_a = 0.2m/s$. With these approximations, the PMV equation from (4-4) can be expressed as a function of Temperature T_{rm} and water vapour pressure ρ_a, and given by

$$PMV_{rm} = at_r + b\rho_a - c \tag{4-6}$$

where a, b and c are Rohles' experimental coefficients, and are dependent on the gender of the occupants. For a male occupant, $a = 0.212$, $b = 0.293$, $c = 5.949$ and for a female it is $a = 0.275$, $b = 0.255$, $c = 8.62$. This modified PMV index given in (4-6) was used in the generation of the cost function of the MPC.

Cost function for set-point controller

In this section, the controller formulation is based on the work done in [37]. For the formation of a higher level controller, an augmented state space matrix with the PI controller states and

the plant states is formulated, which yields an augmented state vector $\bar{x} = \begin{bmatrix} x & x_c \end{bmatrix}^T$, where $x_c(k) \in \mathbb{R}^4$ represents the PI controller states. Substituting for input $u_c(k)$ in (4-2),

$$\begin{aligned} \bar{x}(k+1) &= A_{in}\bar{x}(k) + B_{in}e(k) \\ u_c(k) &= C_{in_u}\bar{x}(k) + D_{in_u}e(k) \\ y(k) &= C_{in_y}\bar{x}(k) + D_{in_y}e(k) \end{aligned} \tag{4-7}$$

with $u_c(k) \in \mathbb{R}^4$ being the PI controller inputs and $e(k) \in \mathbb{R}^{4\times 1}$ being the error vector and

$$\begin{aligned} A_{in} &= \begin{bmatrix} A & BC_c \\ 0 & A_c \end{bmatrix} \quad B_{in} = \begin{bmatrix} BD_c \\ B_c \end{bmatrix} \\ C_{in_u} &= \begin{bmatrix} 0 & C_c \end{bmatrix} \quad D_{in_u} = D_c \\ C_{in_y} &= \begin{bmatrix} C & DC_c \end{bmatrix} \quad D_{in_y} = DD_c. \end{aligned}$$

Substituting back for $e(k)$, the overall closed-loop equations with PI controllers are obtained.

$$\begin{aligned} A_{out} &= A_{in} - B_{in}(I + D_{in_y})^{-1}C_{in_y} \\ B_{out} &= B_{in} - B_{in}(I + D_{in_y})^{-1}D_{in_y} \end{aligned}$$

$$\begin{aligned} C_{out_u} &= C_{in_u} - D_{in_y}(I + D_{in_y})^{-1}C_{in_u} \\ D_{out_u} &= D_{in_u} - D_{in_u}(I + D_{in_y})^{-1}D_{in_u} \\ C_{out_y} &= (I + D_{in_y})^{-1}C_{in_y} \\ D_{out_y} &= (I + D_{in_y})^{-1}D_{in_y} \end{aligned} \tag{4-8}$$

which finally gives us the complete state space dynamics of the discrete-time closed-loop system (the blue dashed box in Fig. 4-2)

$$\begin{aligned} \bar{x}(k+1) &= A_{out}\bar{x}(k) + B_{out}w(k) \\ u_c(k) &= C_{out_u}\bar{x}(k) + D_{out_u}w(k) \\ y(k) &= C_{out_y}\bar{x}(k) + D_{out_y}w(k) \end{aligned} \tag{4-9}$$

where $w(k)$ is a vector of set-point temperatures with $w = [T_{set_1}\, T_{set_2}\, T_{set_3}\, T_{set_4}]^T$. The numerical values of the closed loop matrices that were calculated for this design have been attached in the Appendix.

Using (4-6) and the closed loop state space derived in (4-9), the optimization problem for the formulation of the MPC is as follows:

$$\begin{aligned} \underset{\tilde{w}(k_p),\tilde{y}(k_p)}{\text{minimize}} \sum_{k=0}^{N_p-1} \Bigg(& \underbrace{(||K_y(y(k) - w(k))||_\infty}_{\text{error minimization}} + \\ & \underbrace{||K_{pmv}(PMV_{rm}(k))||_1}_{\text{comfort}} + \underbrace{||K_u\Delta u||_1}_{\text{input minimization}} \Bigg) \\ \text{subject to: Equation}(4-9) & \\ -0.2 \leq & PMV_{rm}(k) \leq 0.2, \\ 0.001 \leq u(k) \leq 0.03 & \\ 18 \leq & y \leq 30 \end{aligned} \tag{4-10}$$

where $n = \{0, 1\}$ indicates occupancy status, s is a slack variable. A prediction horizon of $N_p = 4$ is chosen for the optimization problem. Control input is generated every 10 minutes, to make it as close as possible to a real life scenario. For this work, values chosen were $K_y = \text{diag}([1\,1\,1\,1])$, $K_{pmv} = \text{diag}([0.5\,0.5\,0.5\,0.5])$ and $K_u = \text{diag}([0.1\,0.1\,0.1\,0.1])$ based on trial and error. Since the parameters for the optimization were of similar order, there was no need for scaling of the objective function.

The infinity norm ($||.||_\infty$) is chosen to minimize the first term, so that the worst case error is minimized. The one norm ($||.||_1$) is used for changes in the input and in the PMV. As can be seen from 4-10, it is seen that the constraints of the MPC are computed dynamically to ensure that there is minimum fresh air input when there is no occupancy, thereby minimizing the overall efficiency of the system.

4-3 Simulation of proposed strategy

A model of the building was constructed from (4-1) with the controller structure controlling the test case as described by the physical equations. The MPC problem was formulated and solved using YALMIP [38]. The inlet air temperature has been selected as 16 $°C$ as suggested by the facility management. To ensure that there is no accumulation of CO_2 in the room, there is a minimal airflow input of 0.001 kg/s when there is an occupant in the room.

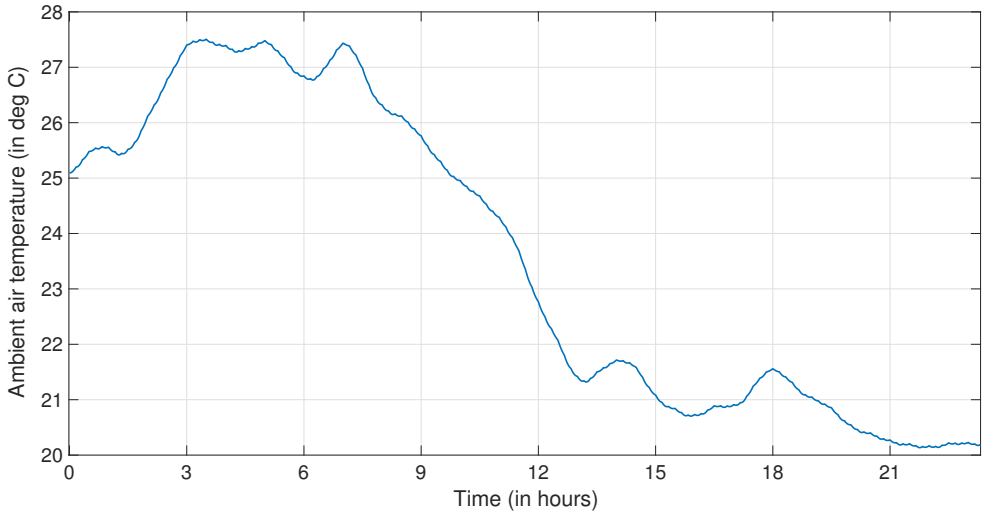

Figure 4-3: Ambient weather temperature for June 19th, 2017

The proposed MPC+Autotuned PI strategy is simulated in . To highlight energy savings, this strategy is compared with a baseline control that tracks a constant set point of 24$°C$ and where no knowledge of the occupancy is known. Simulations are run for a span of 24 hours, with weather profile taken from June $19th, 2017$, as shown in Fig. 4-3. The tracking performance of the controller when the setpoint is constant is shown in Figure 4-4.

Figs. 4-5 and 4-6 show the temperature tracking for 2 rooms (the other room and the corridor have a similar behavior to the one shown here and are shown in the appendix). The

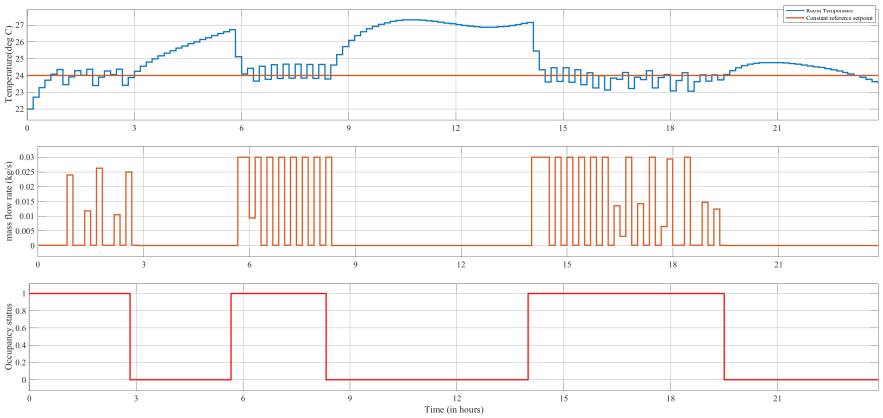

Figure 4-4: Controller performance for tracking of constant setpoint, corridor

maximum error in set-point tracking when the occupants are in the room is around $\pm 1°C$, even accounting for quantization error in measurement by sensors.

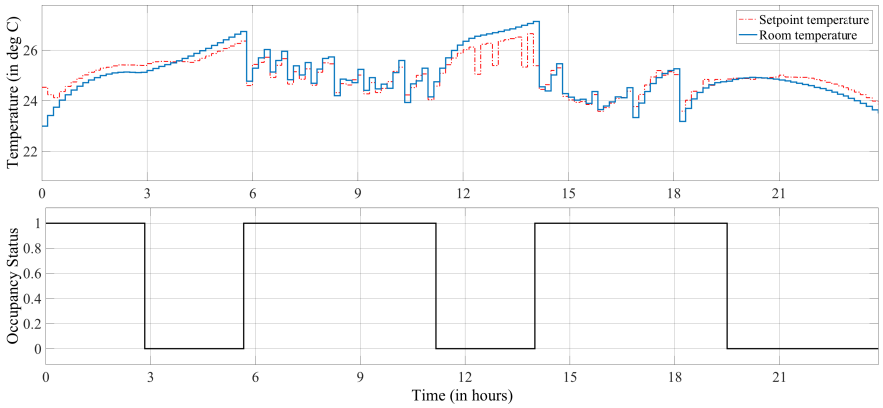

Figure 4-5: Set-point tracking, Room 1

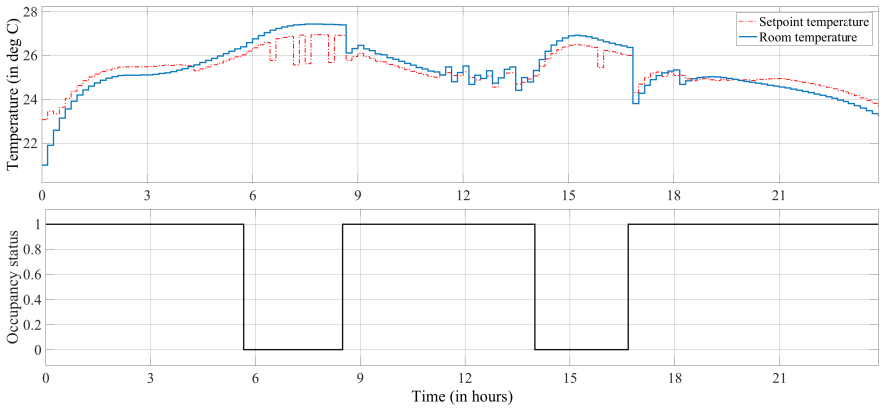

Figure 4-6: Set-point tracking, Room 2

Figs. 4-7 and 4-8 show the PMV profile for 2 rooms (as with the previous case, the other room and corridor have similar behavior to the one shown here and have been attached in

the Appendix). When occupants are present in a room, it can be seen that the setpoints are dynamically changed to ensure PMV is almost always maintained within ±0.2, falling under 'Class A' of thermal comfort criterion, indicating maximum possible thermal comfort [39].

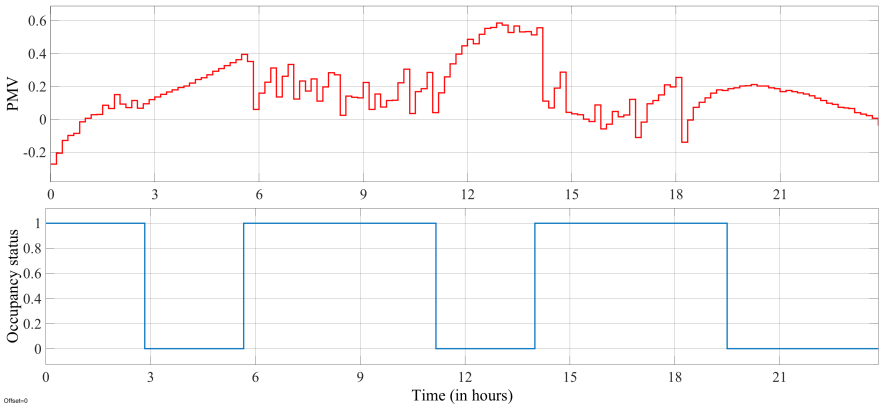

Figure 4-7: Evolution of PMV vs Occupancy, Room 1

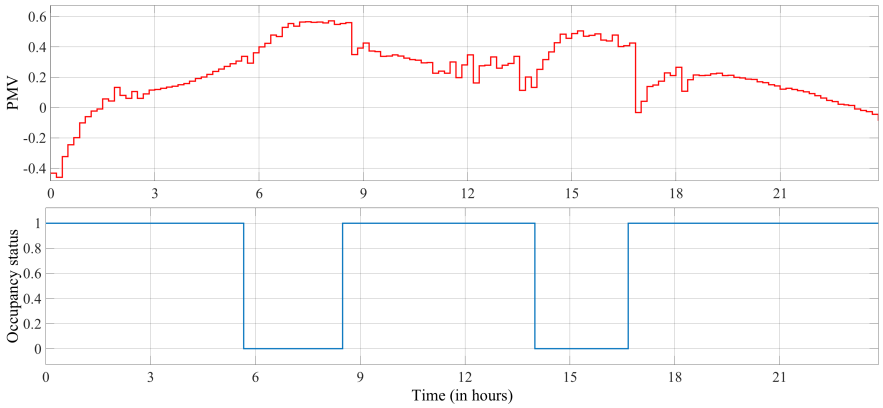

Figure 4-8: Evolution of PMV vs Occupancy, Room 2

When the occupants are not present in the room, the controllers are switched off, ensuring that there is no air flow. In this case, temperature evolution in the room/corridor is mainly due to conduction through the walls and windows. The variation of input airflow and temperature and along with the occupancy is shown in Figs. 4-9 and 4-10. Once the user is back in the room, the optimal set-points are once again generated to ensure maximum comfort.

Table 4-4 shows the comparison of power consumption for the variable supply fan for the baseline PI strategy with the PI with MPC. For the calculation of power, a static pressure of $\Delta P = 500\ Pa$ and ideal efficiency is assumed. Results show potential for good tracking with reduced cooling load. It can be seen that while the optimization only accounted for reduction in fan power, this will also automatically mean that the pump and chiller load will also be reduced.

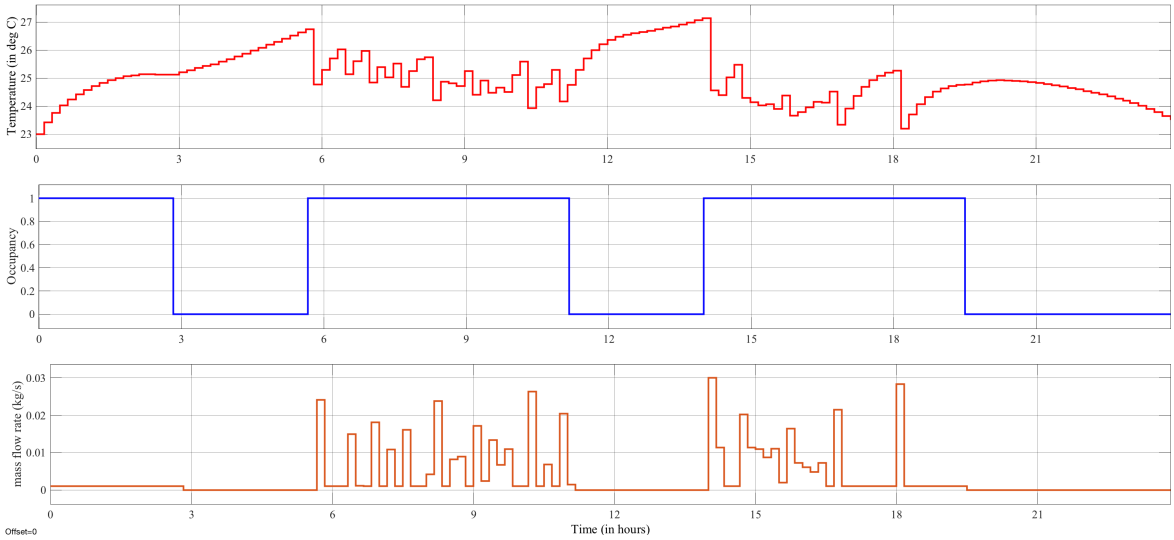

Figure 4-9: Evolution of temperature and mass flow rate vs occupancy, room 1

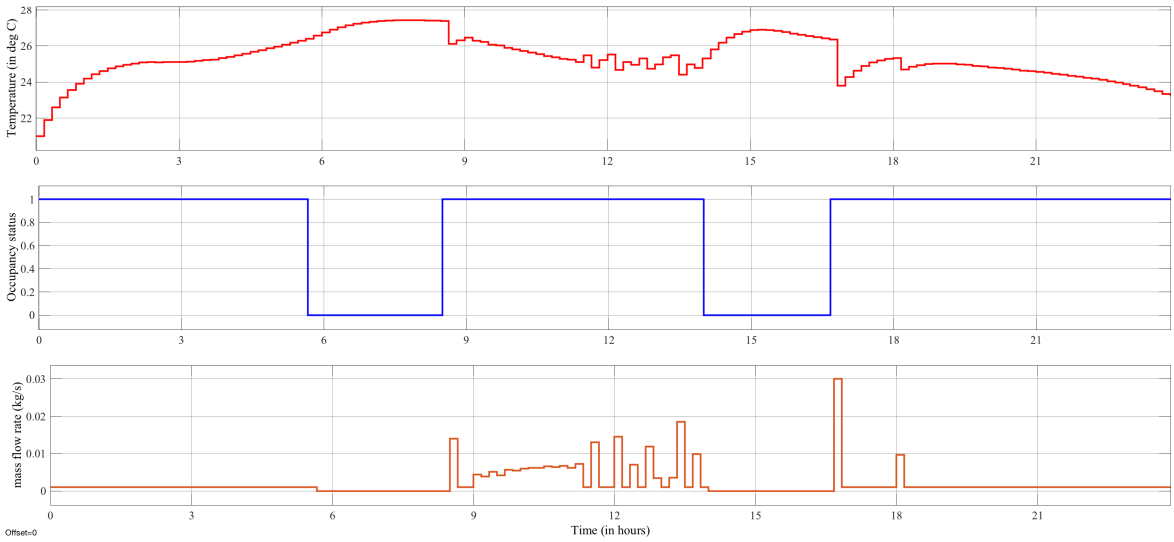

Figure 4-10: Evolution of temperature and mass flow rate vs occupancy, room 2

Table 4-4: Total energy consumption in [kWh] for a simulation length of one day

Controller	Total Airflow (kg)	Energy Consumption [kW]
Baseline PI	1132.5	12.770
MPC with optimized PI	1877.1	7.703 (-39.67%)

4-4 Summary

A controller structure that optimizes the airflow input into the individual rooms based on comfort, energy consumption and occupancy schedule has been constructed. Incorporation of the PMV into the optimization has ensured that the controller is modelled around the user

and therefore the set-points could be dynamically adjusted according to external weather and clothing conditions of the user. The proposed strategy is also a proof-of-concept of how the decoupled models that were constructed in chapters 2 and 3 could be used to created an integrated control structure. The advantage of the proposed controller structure is that it can be scaled to a large number of rooms, and potentially even a whole building.

Chapter 5

Conclusions and Recommendations

5-1 Conclusions

Referring back to the research questions that were posed in Chapter 1-4, we make the following conclusions in this thesis:

The aim of this MSc thesis was to address the following aspects:

- *Is it possible to reformulate the bilinear dynamics of temperature, humidity and CO_2 in a linear way so that linear identification techniques can be implemented ?*

  The physical equations describing the dynamics of temperature, CO_2 and humidity were restructured in an ARMAX format. The temperature dynamics were validated with experimental data showing a good fit, even for limited datasets.

- *Can a control strategy be developed based on the developed models whose control action is based on the external weather conditions and thermal comfort of the users?*

  A hierarchical upper layer MPC with lower layer PI was formulated and simulated by incorporating a linearized version of the PMV index thereby customizing the control output according to the comfort of each user.

- *Can the control strategy be customized for occupant in each room so that rooms are heated/cooled only when the occupant is present in the room?*

  The control strategy accounted for incorporating the occupancy status in the optimization to ensure that heating/cooling was done only when the occupants were present in the room.

5-2 Recommendations and Future Work

For the purposes of this thesis, it was only possible to validate the temperature dynamics due to limited availability of the datasets. Therefore, it leaves an opportunity to validate the

models for CO_2 and humidity dynamics. With information from these dynamics, it would be possible to incorporate these dynamics, which have currently been assumed as a constant, into the predictive controller design. Furthermore, with extended datasets, the model could also be evaluated for its accuracy over various seasons.

The ARX/ARMAX based approach gives a simple and intuitive understanding of the physics of the system in discrete time. In the case where the input mass flow rate was available as an measurement, it would also be possible to estimate the parameters of the bilinear model for temperature evolution using Nonlinear ARX (NLARX) structure.

In Section 2-3, the model was formulated with the assumption that the windows are always closed. However, this not true in real world conditions, where users tend to open/close windows based on external weather conditions and dim lighting. Therefore, under controlled conditions, a Hybrid Piecewise Affine (PWA) could be created which could capture both the effects based on the window opening status. Similar models could be created for humidity and CO_2 as well.

The test case considered for a hierarchical control algorithm only considers a simplified cooling case, a more realistic future goal would be to extend the integrated control oriented model to a heating test case as well, so that overall system gains could be tested. Furthermore, the test case accounts for an ideal room where there is very high thermal mass and therefore the effect of the external temperature is neglected for simplicity. Modelling the system while estimating the disturbances, with say, a Kalman filter, would prove an even more realistic model for control purposes.

With increasing complexity in building model, computing the predictive controller action might become computationally expensive. There are 2 ways to overcome this, the first is to use faster numerical solvers. The second would require the use of a Decentralized MPC (DMPC), similar to the proposal by [40], but with the incorporation of thermal comfort indices as done in this work, and weather forecasts, as was done in [27].

Appendix A

System matrices and controller output for control system

A-1 System Matrices

This section highlights the closed loop system matrices that were developed for the controller design in Chapter 4:

A_out =

$$\begin{bmatrix} -1.0067 & 0 & 0 & 0 & 2.0067 & 0 & 0 & 0 \\ 0 & -1.0067 & 0 & 0 & 0 & 2.0067 & 0 & 0 \\ 0 & 0 & -1.0067 & 0 & 0 & 0 & 2.0067 & 0 \\ 0 & 0 & 0 & -1.0067 & 0 & 0 & 0 & 2.0067 \\ 0 & 0 & 0 & 0 & -7.0215 & 0.0005 & 0.0005 & 0.0005 \\ 0 & 0 & 0 & 0 & 0.0005 & -6.0473 & 0.0005 & 0.0005 \\ 0 & 0 & 0 & 0 & 0.0003 & 0.0003 & -2.9892 & 0.0003 \\ 0 & 0 & 0 & 0 & -0.2289 & -0.1927 & -0.0789 & -3.0274 \end{bmatrix}$$

B_out =

$$\begin{bmatrix} -2.0067 & 0 & 0 & 0 \\ 0 & -2.0067 & 0 & 0 \\ 0 & 0 & -2.0067 & 0 \\ 0 & 0 & 0 & -2.0067 \\ 7.8144 & -0.0005 & -0.0005 & -0.0005 \\ -0.0005 & 6.8401 & -0.0005 & -0.0005 \\ -0.0003 & -0.0003 & 3.7821 & -0.0003 \\ 0.2903 & 0.2540 & 0.1403 & 3.8202 \end{bmatrix}$$

$$\text{C\_out\_u} = 1.0 \times 10^{-7} \times \begin{bmatrix} 0.3846 & 0.3846 & 0.3846 & 0.3846 & 0 & 0 & 0 & 0 \\ 0.3779 & 0.3779 & 0.3779 & 0.3779 & 0 & 0 & 0 & 0 \\ 0.3712 & 0.3712 & 0.3712 & 0.3712 & 0 & 0 & 0 & 0 \\ 0.3712 & 0.3712 & 0.3712 & 0.3712 & 0 & 0 & 0 & 0 \end{bmatrix}$$

$$\text{D\_out\_u} = \begin{bmatrix} -0.1725 & 0 & 0 & 0 \\ 0 & -0.1469 & 0 & 0 \\ 0 & 0 & -0.1221 & 0 \\ 0 & 0 & 0 & -0.1221 \end{bmatrix}$$

$$\text{C\_out\_y} = \begin{bmatrix} 0 & 0 & 0 & 0 & 1 & 0 & 0 & 0 \\ 0 & 0 & 0 & 0 & 0 & 1.0000 & 0 & 0 \\ 0 & 0 & 0 & 0 & 0 & 0 & 1 & 0 \\ 0 & 0 & 0 & 0 & 0 & 0 & 0 & 1 \end{bmatrix}$$

$$\text{D\_out\_y} = \begin{bmatrix} 0 & 0 & 0 & 0 \\ 0 & 0 & 0 & 0 \\ 0 & 0 & 0 & 0 \\ 0 & 0 & 0 & 0 \end{bmatrix}$$

Figure A-2 shows the setpoint tracking for Room 3. Figures A-3 and A-4 show the evolution of PMV with Occupancy for Room 3 and the Corridor. Finally, Figures A-5 and A-6 show the evolution of inputs with temperature and occupancy.

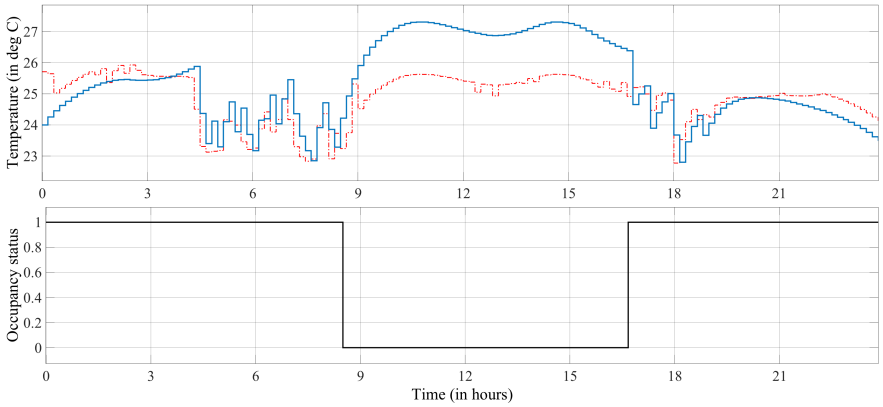

Figure A-1: Set-point tracking, Room 3

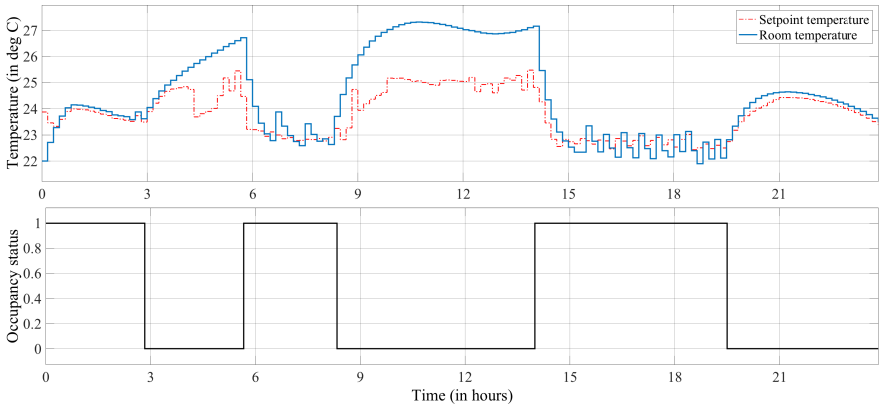

Figure A-2: Set-point tracking, Room 3

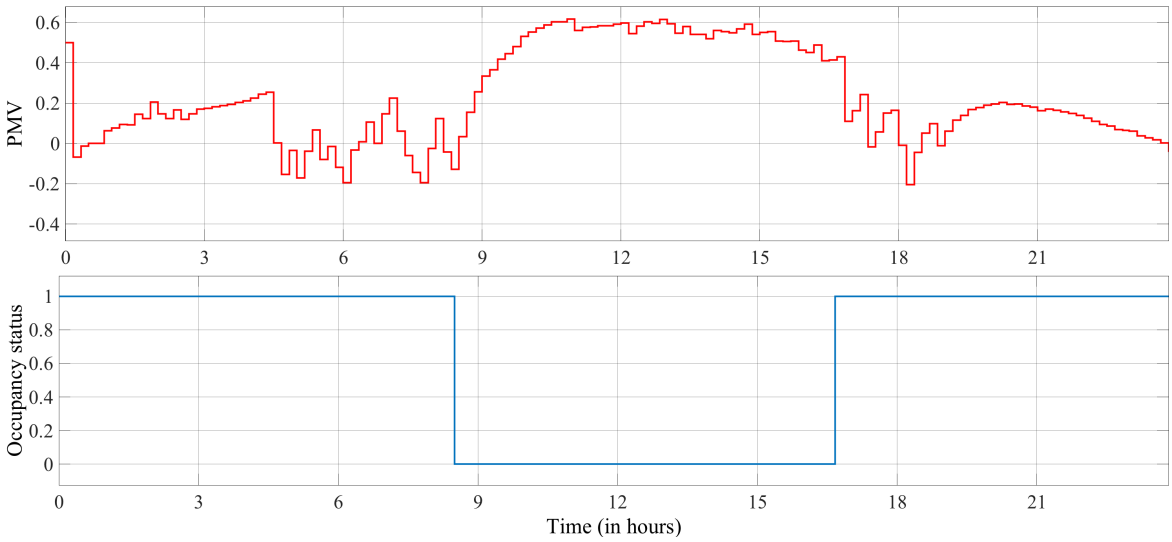

Figure A-3: Evolution of PMV vs Occupancy, Room 3

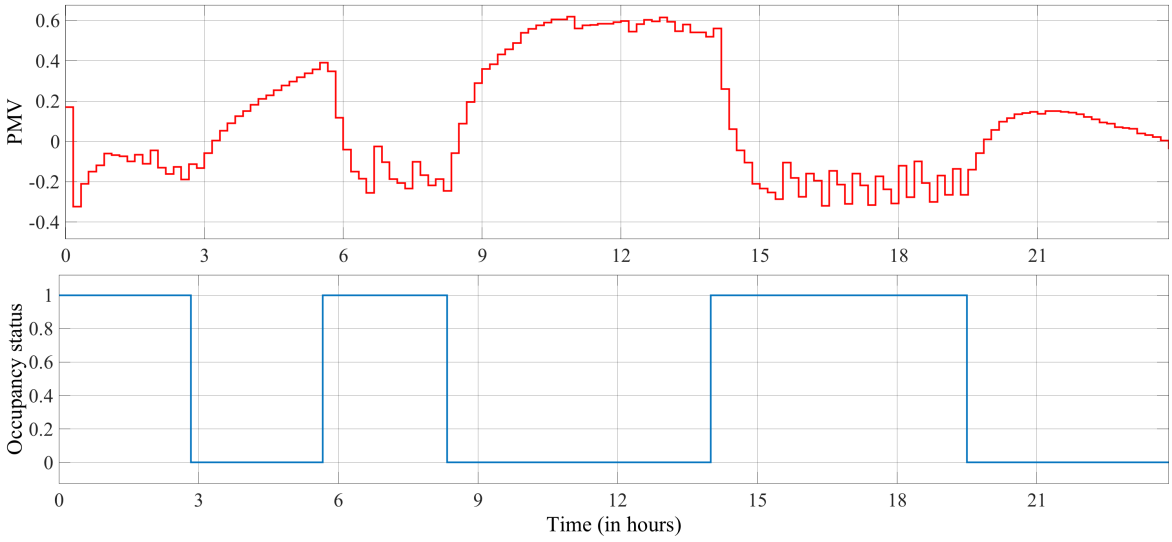

Figure A-4: Evolution of PMV vs Occupancy, Corridor

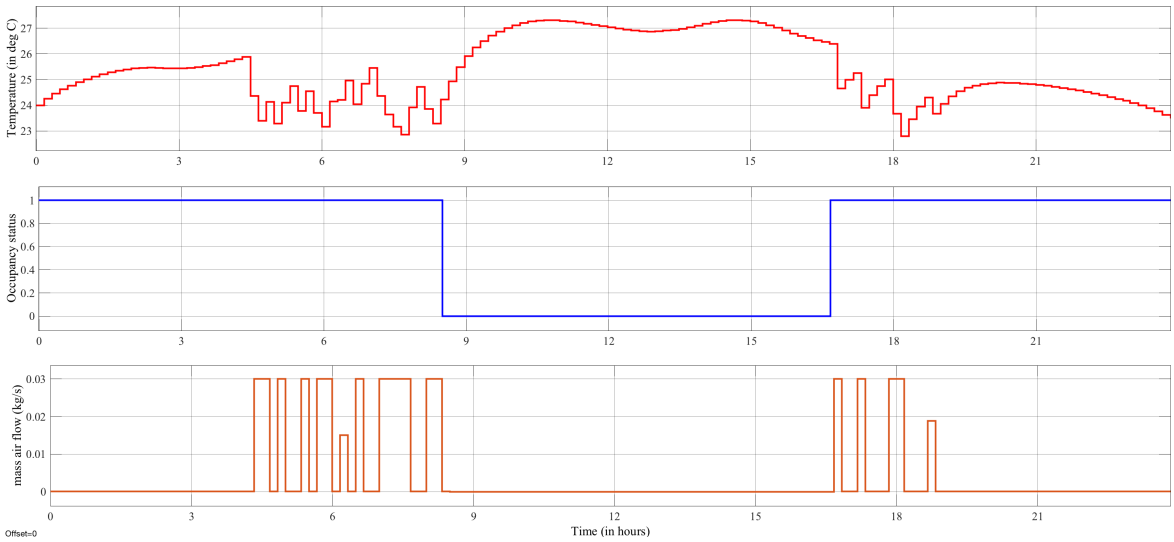

Figure A-5: Evolution of temperature and mass flow rate vs occupancy, room 3

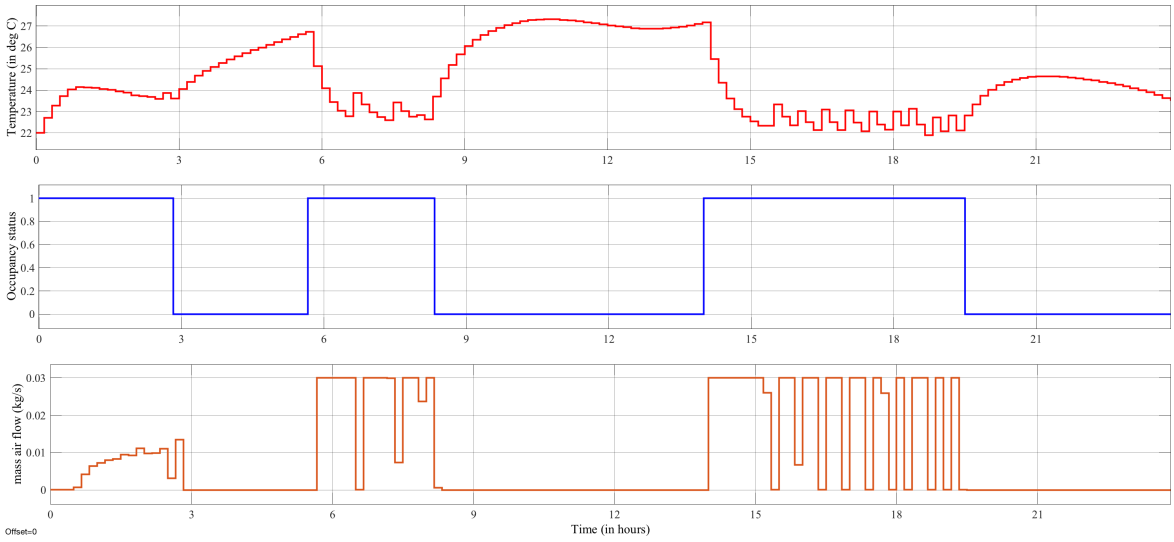

Figure A-6: Evolution of temperature and mass flow rate vs occupancy, corridor

Appendix B

Preliminaries

B-1 VAV HVAC systems

B-1-1 VAV Air Handling Unit

The Air Handling Unit is responsible for filtering, mixing, supplying and exhausting air throughout the building. A large building typically has multiple AHUs to facilitate mixing individually for each floor. The return air from the building is mixed with outside air in the mixing box. This ratio is dependant on the current temperature, humidity and CO2 levels of the return and supply air. The ratio of mixing is controlled through the use of dampers. The dampers mix a ratio of outside and return air to ensure temperature and indoor air quality levels are satisfied. Once the air has been mixed and passed through the filters, it must be conditioned before it enters the spaces within the building.

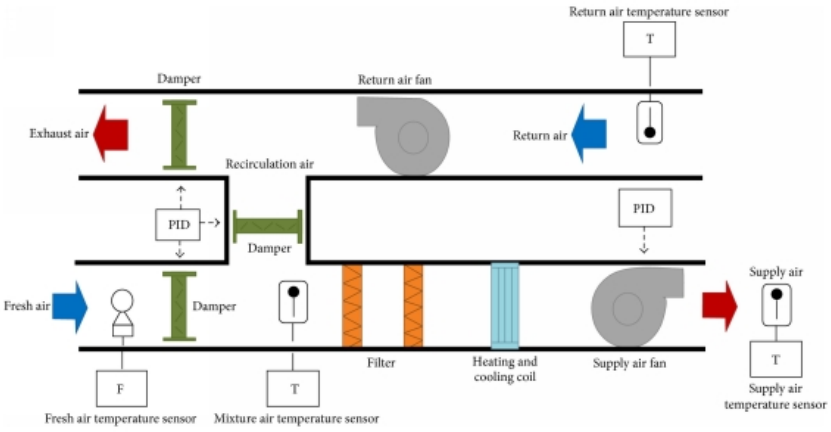

Figure B-1: Schematic of a typical VAV AHU [6]

The next part of the air handling unit is the heat recovery unit. The primary function of the heat recovery unit is to transfer moisture and heat from the exhaust air to the supply air. After travelling through the heat recovery unit, the air passes through the condenser coils, heating coils, and cooling coils. The condensor coil is used to condense any excess moisture that maybe present in the incoming air by passing the incoming air through a refrigerant. This excess moisture, condenses and its drained from the system. The heating and cooling. Depending on the demand and current conditions within the room, air is heated or cooled using heating or cooling coils respectively. Now we can say that the incoming air has been sufficiently conditioned and can be sent to the occupant space. This is done so through the use of creating a pressure differential using suction fans, also commonly known in HVAC terminology as supply fans. These supply fans push the conditioned air to the supply ductwork and eventually the VAV boxes. A simple schematic of a VAV Air Handling Unit is shown in Figure B-1.

B-1-2 VAV Box

The VAV box consists of a motor operated damper, a reheat coil and a temperature sensor. With inputs from the temperature sensor, the VAV box regulates the flow of conditioned air into the occupied zone via control of the damper. Generally, there is a standard amount of ventilation that has to be provided to a certain space and according to these requirements, a minimum amount of fresh air has to be introduced into the occupant space. When the volume of air from the supply duct needed to cool the zone is lesser than the fresh air requirement, the reheat coil slightly heats up the fresh air entering the space so that the conditioned air can still be supplied without adversely affecting the temperature of the room, i.e. there is no over-cooling or over-heating of the occupant space. Finally, the occupant zone also consists of an exhaust ductwork which has a suction fan, also called as exhaust fan, which sucks air from the occupant space and sends it back to the AHU for mixing and/or vent it back to the external environment.

Bibliography

[1] E. Efficiency, "Buildings energy data book," *US Department of Energy. http://buildingsdatabook. eere. energy. gov/. John Dieckmann is a director and Alissa Cooperman is a technologist in the Mechanical Systems Group of TIAX, Cambridge, Mass. James Brodrick, Ph. D., is a project manager with the Building Technologies Program, US Department of Energy, Washington, DC*, 2009.

[2] S. Goyal, P. Barooah, and T. Middelkoop, "Experimental study of occupancy-based control of hvac zones," *Applied Energy*, vol. 140, pp. 75–84, 2015.

[3] A. Kusiak, F. Tang, and G. Xu, "Multi-objective optimization of hvac system with an evolutionary computation algorithm," *Energy*, vol. 36, no. 5, pp. 2440–2449, 2011.

[4] M. Maasoumy and A. Sangiovanni-Vincentelli, "Total and peak energy consumption minimization of building hvac systems using model predictive control," *IEEE Design & Test of Computers*, vol. 29, no. 4, pp. 26–35, 2012.

[5] K. Weekly, N. Bekiaris-Liberis, M. Jin, and A. M. Bayen, "Modeling and estimation of the humans' effect on the co 2 dynamics inside a conference room," *IEEE Transactions On Control Systems Technology*, vol. 23, no. 5, pp. 1770–1781, 2015.

[6] H. Wang, "Application of residual-based ewma control charts for detecting faults in variable-air-volume air handling unit system," *Journal of Control Science and Engineering*, vol. 2016, p. 8, 2016.

[7] L. Pérez-Lombard, J. Ortiz, and C. Pout, "A review on buildings energy consumption information," *Energy and buildings*, vol. 40, no. 3, pp. 394–398, 2008.

[8] I. Knight, "Assessing electrical energy use in hvac systems." http://www.rehva.eu/fileadmin/hvac-dictio/01-2012/assessing-electrical-energy-use-in-hvac-systems_rj1201.pdf, 2012.

[9] A. Wemhoff, "Calibration of hvac equipment pid coefficients for energy conservation," *Energy and Buildings*, vol. 45, pp. 60–66, 2012.

[10] M. Schicktanz and T. Nunez, "Modelling of an adsorption chiller for dynamic system simulation," *International Journal of Refrigeration*, vol. 32, no. 4, pp. 588–595, 2009.

[11] M. Teitel, A. Levi, Y. Zhao, M. Barak, E. Bar-lev, and D. Shmuel, "Energy saving in agricultural buildings through fan motor control by variable frequency drives," *Energy and Buildings*, vol. 40, no. 6, pp. 953–960, 2008.

[12] J. Koh, J. Z. Zhai, and J. A. Rivas, "Comparative energy analysis of vrf and vav systems under cooling mode," in *ASME 3rd international conference on energy sustainability, ES2009; San Francisco, United States, 19*, vol. 1, pp. 411–418, 2009.

[13] G. P. Henze, A. R. Florita, M. J. Brandemuehl, C. Felsmann, and H. Cheng, "Advances in near-optimal control of passive building thermal storage," *Journal of Solar Energy Engineering*, vol. 132, no. 2, p. 021009, 2010.

[14] S. Wang and Z. Ma, "Supervisory and optimal control of building hvac systems: A review," *HVAC&R Research*, vol. 14, no. 1, pp. 3–32, 2008.

[15] Z. Ma, S. Wang, X. Xu, and F. Xiao, "A supervisory control strategy for building cooling water systems for practical and real time applications," *Energy Conversion and Management*, vol. 49, no. 8, pp. 2324–2336, 2008.

[16] N. N. S. Moujaes, "A cost-effective operating strategy to reduce energy consumption in a hvac system," *International Journal of Energy Research*, vol. 32, pp. 543–558, 2008.

[17] P. Ferreira, A. Ruano, S. Silva, and E. Conceicao, "Neural networks based predictive control for thermal comfort and energy savings in public buildings," *Energy and Buildings*, vol. 55, pp. 238–251, 2012.

[18] A. Kusiak and G. Xu, "Modeling and optimization of hvac systems using a dynamic neural network," *Energy*, vol. 42, no. 1, pp. 241–250, 2012.

[19] N. Nassif, "Modeling and optimization of hvac systems using artificial neural network and genetic algorithm," in *Building Simulation*, vol. 7, pp. 237–245, Springer, 2014.

[20] G. Mustafaraj, J. Chen, and G. Lowry, "Development of room temperature and relative humidity linear parametric models for an open office using bms data," *Energy and Buildings*, vol. 42, no. 3, pp. 348–356, 2010.

[21] M. Maasoumy, "Modeling and optimal control algorithm design for hvac systems in energy efficient buildings," 2014.

[22] R. Bălan, J. Cooper, K.-M. Chao, S. Stan, and R. Donca, "Parameter identification and model based predictive control of temperature inside a house," *Energy and Buildings*, vol. 43, no. 2, pp. 748–758, 2011.

[23] S. Wu and J.-Q. Sun, "A physics-based linear parametric model of room temperature in office buildings," *Building and Environment*, vol. 50, pp. 1–9, 2012.

[24] F. Scotton, L. Huang, S. A. Ahmadi, and B. Wahlberg, "Physics-based modeling and identification for hvac systems?," in *Control Conference (ECC), 2013 European*, pp. 1404–1409, IEEE, 2013.

[25] G. S. Brager and R. De Dear, "Climate, comfort, & natural ventilation: a new adaptive comfort standard for ashrae standard 55," 2001.

[26] ASHRAE, "ANSI/ASHRAE standard 55-2010: thermal environmental conditions for human occupancy," *American Society of Heating, Refrigerating and air-Conditioning Engineers*, 2010.

[27] F. Oldewurtel, A. Parisio, C. N. Jones, D. Gyalistras, M. Gwerder, V. Stauch, B. Lehmann, and M. Morari, "Use of model predictive control and weather forecasts for energy efficient building climate control," *Energy and Buildings*, vol. 45, pp. 15–27, 2012.

[28] B. Dong and K. P. Lam, "A real-time model predictive control for building heating and cooling systems based on the occupancy behavior pattern detection and local weather forecasting," in *Building Simulation*, vol. 7, pp. 89–106, Springer, 2014.

[29] M. Pcolka, E. Zacekova, R. Robinett, S. Celikovsky, and M. Sebek, "Economical nonlinear model predictive control for building climate control," in *American Control Conference (ACC), 2014*, pp. 418–423, IEEE, 2014.

[30] S. Baldi, S. Yuan, P. Endel, and O. Holub, "Dual estimation: Constructing building energy models from data sampled at low rate," *Applied Energy*, vol. 169, pp. 81–92, 2016.

[31] A. Parisio, L. Fabietti, M. Molinari, D. Varagnolo, and K. H. Johansson, "Control of hvac systems via scenario-based explicit mpc," in *Decision and Control (CDC), 2014 IEEE 53rd Annual Conference on*, pp. 5201–5207, IEEE, 2014.

[32] A. Standard, "Standard 62-1989, ventilation for acceptable indoor air quality," *Atlanta*, 1989.

[33] F. Lauro, L. Longobardi, and S. Panzieri, "An adaptive distributed predictive control strategy for temperature regulation in a multizone office building," in *Intelligent Energy Systems (IWIES), 2014 IEEE International Workshop on*, pp. 32–37, IEEE, 2014.

[34] P. Fanger, "Calculation of thermal comfort, introduction of a basic comfort equation," *ASHRAE transactions*, vol. 73, no. 2, pp. III–4, 1967.

[35] I. T. Michailidis, S. Baldi, M. F. Pichler, E. B. Kosmatopoulos, and J. R. Santiago, "Proactive control for solar energy exploitation: A german high-inertia building case study," *Applied Energy*, vol. 155, pp. 409–420, 2015.

[36] F. H. Rohles Jr, "Thermal sensations of sedentary man in moderate temperatures," *Human factors*, vol. 13, no. 6, pp. 553–560, 1971.

[37] M. Klaučo, *Modeling of the Closed-loop System with a Set of PID controllers.* Slovak University of Technology in Bratislava, Radlinského 9, 812 37 Bratislava, November 2016.

[38] J. Löfberg, "Yalmip : A toolbox for modeling and optimization in matlab," in *In Proceedings of the CACSD Conference*, (Taipei, Taiwan), 2004.

[39] E. Iso, "7730: 2005," *Ergonomics of the thermal environment-Analytical determination and interpretation of thermal comfort using calculation of the PMV and PPD indices and local thermal comfort criteria*, 2005.

[40] Y. Ma, G. Anderson, and F. Borrelli, "A distributed predictive control approach to building temperature regulation," in *American Control Conference (ACC), 2011*, pp. 2089–2094, IEEE, 2011.